

Influence of untrapped electrons on the sideband instability in a helical wiggler free electron laser

Ronald C. Davidson^{a)}

Science Applications International Corporation, Boulder, Colorado 80302

Jonathan S. Wurtele

Plasma Fusion Center, Massachusetts Institute of Technology, Cambridge, Massachusetts 02139

(Received 30 September 1986; accepted 3 June 1987)

The detailed influence of an untrapped-electron population on the sideband instability in a helical wiggler free electron laser is investigated for small-amplitude perturbations about a constant-amplitude ($\hat{a}_s^0 = \text{const}$) primary electromagnetic wave with slowly varying equilibrium phase δ_s^0 . A simple model is adopted in which all of the trapped electrons are deeply trapped, and the equilibrium motion of the untrapped electrons (assumed monoenergetic) is only weakly modulated by the ponderomotive potential. The theoretical model is based on the single-particle orbit equations together with Maxwell's equations and appropriate statistical averages. Moreover, the stability analysis is carried out in the ponderomotive frame, which leads to a substantial simplification in deriving the dispersion relation. Detailed stability properties are investigated over a wide range of dimensionless pump strength $\Omega_B/\Gamma_b c k_0$ and fraction of untrapped electrons $f_u = \hat{n}_u/\hat{n}_b$. When both trapped and untrapped electrons are present, there are generally two types of unstable modes, referred to as the *sideband* mode, and the *untrapped-electron* mode. For $f_u = 0$, only the sideband instability is present. As f_u is increased, the growth rate of the sideband instability decreases, whereas the growth rate of the untrapped-electron mode increases until only the untrapped-electron mode is unstable for $f_u = 1$. It is found that the characteristic maximum growth rate of the most unstable mode varies by only a small amount over the entire range of f_u from $f_u = 0$ (no untrapped electrons) to $f_u = 1$ (no trapped electrons). The present analysis suggests that the linear and nonlinear evolution of the beam electrons and radiation field may be substantially modified by the presence of an untrapped-electron component when $f_u \gtrsim 0.2$.

I. INTRODUCTION

Free electron lasers (FEL's),¹⁻⁴ as evidenced by the growing experimental⁵⁻²² and theoretical²³⁻⁷⁰ literature on this subject, can be effective sources for coherent radiation generation by intense relativistic electron beams. Recent theoretical studies have included investigations of nonlinear effects²³⁻⁴⁷ and saturation mechanisms, the influence of finite geometry on linear stability properties,⁴⁸⁻⁵³ novel magnetic field geometries for radiation generation,^{48,54-58} and fundamental studies of stability behavior.⁵⁹⁻⁷⁰ One topic of considerable practical interest is the sideband instability³⁶ which results from the bounce motion of electrons trapped in the (finite-amplitude) ponderomotive potential. Both kinetic²³⁻²⁵ and single-particle³⁶⁻⁴⁷ models of the sideband instability have been developed, and numerical simulations³⁹⁻⁴⁷ have been carried out. However, with the exception of the recent kinetic formalism developed by Davidson *et al.*,²³⁻²⁵ the analytical treatments have consistently neglected the effects of any untrapped-electron population.

The purpose of the present analysis is to investigate the detailed influence of untrapped electrons on the sideband instability. Small-amplitude perturbations are assumed about a constant-amplitude ($\hat{a}_s^0 = \text{const}$) primary electro-

magnetic wave with slowly varying equilibrium phase δ_s^0 . Moreover, we adopt a simple model in which all of the trapped electrons are deeply trapped, and the equilibrium motion of the untrapped electrons (assumed monoenergetic) is only weakly modulated by the ponderomotive potential. The theoretical model (Sec. II) is based on the single-particle orbit equations together with Maxwell's equations and appropriate statistical averages.^{36,37} Like our recent treatment³⁷ of the sideband instability (which neglects the effects of untrapped electrons), the present analysis is carried out in the ponderomotive frame, which leads to a substantial simplification in the analysis.

The theoretical model and assumptions are described in Sec. II. A tenuous, relativistic electron beam propagates through a constant-amplitude helical wiggler magnetic field with wavelength $\lambda_0 = 2\pi/k_0 = \text{const}$, and normalized amplitude $a_w = e\hat{B}_w/mc^2k_0 = \text{const}$ [Eq. (1)]. The model neglects longitudinal perturbations (Compton-regime approximation with $\delta\phi \simeq 0$) and transverse spatial variations ($\partial/\partial x = 0 = \partial/\partial y$). Moreover, the analysis is carried out for the case of finite-amplitude primary electromagnetic wave (ω_s, k_s) with right-circular polarization and slowly varying normalized amplitude $\hat{a}_s(z, t)$ and wave phase $\delta_s(z, t)$ in the Eikonal approximation [Eq. (2)]. A detailed investigation of the sideband instability simplifies considerably if the analysis is carried out in the ponderomotive frame^{37,71,72} moving with velocity $v_p = \omega_s/(k_s + k_0)$. In the

^{a)} Permanent address: Plasma Fusion Center, Massachusetts Institute of Technology, Cambridge, Massachusetts 02139.

ponderomotive frame ("primed" variables), the nonlinear evolution of $\hat{a}_s(z', t')$ and $\delta'_s(z', t')$ is described by Eqs. (5) and (6), and the electron orbits evolve according to Eq. (13).

In Sec. III, the influence of untrapped electrons on the sideband instability is investigated for small-amplitude perturbations about a primary electromagnetic wave with constant amplitude $\hat{a}_s^0 = \text{const}$ (independent of z' and t'). The trapped and untrapped electrons are treated as distinct components. Moreover, the principal assumptions in the present analysis are the following (Sec. III A).

(a) All of the trapped electrons are *deeply* trapped with a sharply defined energy $\gamma'_j = \hat{\gamma}'_T \approx \hat{\gamma}'_- = [1 + (a_w - \hat{a}_s^0)^2]^{1/2}$. This implies that the trapped electrons are spatially localized ("bunched") near the bottom of the ponderomotive potential (Fig. 2). The average density of the trapped electrons in the ponderomotive frame is $\hat{n}'_T = \hat{n}_T/\gamma_p$.

(b) All of the untrapped electrons have a sharply defined energy $\gamma'_j = \hat{\gamma}'_u > \hat{\gamma}'_+ = [1 + (a_w + \hat{a}_s^0)^2]^{1/2}$, where $\hat{\gamma}'_u$ is sufficiently large that the motion of the untrapped electrons is only weakly modulated by the ponderomotive potential (Fig. 2). The average density of the untrapped electrons in the ponderomotive frame is $\hat{n}'_u = \hat{n}_u/\gamma_p$.

(c) Consistent with (a) and (b), we assume that the perturbations are about a quasisteady equilibrium state characterized by $\hat{a}_s^0 = \text{const}$ (independent of z' and t') and $\partial\delta'_s/\partial t' = 0$. However, a slow spatial variation of the equilibrium phase δ'_s is required [Eq. (41)].

Following a discussion of the quasisteady equilibrium state (Sec. III B), we analyze the linearized wave and particle orbit equations (Sec. III C), and derive the dispersion relation (70) for small-amplitude perturbations in the ponderomotive frame (Sec. III D). Here, it is assumed that the perturbed amplitude $\delta\hat{a}_s(z', t')$, the perturbed phase $\delta'_s(z', t')$, etc., vary as $\exp[-i(\Delta\omega')t' + i(\Delta k')z']$, where $\text{Im}(\Delta\omega') > 0$ corresponds to instability (temporal growth). The dispersion relation (70) relates $\Delta\omega'$ to $\Delta k'$ and other system parameters such as \hat{a}_s^0 , k'_p , \hat{n}'_T , \hat{n}'_u , etc.

Finally, in Sec. IV, the dispersion relation (70) is used to investigate detailed properties of the sideband instability including the effects of the untrapped electrons. First, we transform Eq. (70) back to the laboratory-frame frequency $\omega = \omega_s + \Delta\omega$ and wavenumber $k = k_s + \Delta k$ making use of the transformation in Eq. (71) relating $(\Delta\omega, \Delta k)$ to $(\Delta\omega', \Delta k')$. After some algebraic manipulation (Sec. IV A), we find that the dispersion relation (70) can be expressed as Eq. (80) in the laboratory frame. Equation (86), which is equivalent to Eq. (80), constitutes the final dispersion relation in dimensionless variables analyzed numerically in Sec. IV B. We introduce the parameter $f_u = \hat{n}_u/\hat{n}_b$, where $\hat{n}_b = \hat{n}_T + \hat{n}_u$ is the total average beam density in the laboratory frame [Eq. (82)]. For $f_u = \hat{n}_u/\hat{n}_b = 0$, which corresponds to no untrapped electrons ($\hat{n}_u = 0$), Eq. (86) is the familiar dispersion relation for the sideband instability^{37,73} in circumstances where the equilibrium wave phase is slowly varying [Eq. (41)]. For $f_u \neq 0$, however, it is found that the untrapped electrons can significantly modify stability behavior (Sec. IV B). Detailed stability properties are investigated

over a wide range of both the dimensionless pump strength and the fraction of untrapped electrons. When both trapped and untrapped electrons are present, there are generally two types of unstable modes, referred to as the *sideband* mode, and the *untrapped-electron* mode. For $f_u = 0$, only the sideband instability is present. As f_u is increased, the growth rate of the untrapped-electron mode increases until only the untrapped-electron mode is unstable for $f_u = 1$. While the limiting values, $f_u = 0$ and $f_u = 1$, are both unlikely to be achieved experimentally, their inclusion in the present analysis serves two purposes. First, it allows the dispersion relation (86) to be checked in the two limiting cases where stability properties have previously been calculated. Second, it allows us to identify clearly the untrapped-electron mode ($f_u = 1$) and the sideband mode ($f_u = 0$), and thereby calibrate stability properties for the case where both modes are present ($f_u \neq 0$ and $f_u \neq 1$) and synergistic effects are important.

The present analysis indicates that the detailed stability properties are quite different for the two unstable modes. Equally important, however, it is found that the characteristic maximum growth rate of the most unstable mode varies by only a small amount over the entire range of f_u from $f_u = 0$ (no untrapped electrons) to $f_u = 1$ (no trapped electrons).

II. THEORETICAL MODEL AND ASSUMPTIONS

A. Basic equations and assumptions

A tenuous, relativistic electron beam propagates in the z direction through a constant-amplitude helical wiggler magnetic field with wavelength $\lambda_0 = 2\pi/k_0 = \text{const}$, normalized amplitude $a_w = e\hat{B}_w/mc^2k_0 = \text{const}$, and vector potential specified by

$$\mathbf{A}_w(\mathbf{x}) = -(mc^2/e)a_w(\cos k_0z \mathbf{e}_x + \sin k_0z \mathbf{e}_y). \quad (1)$$

The model neglects longitudinal perturbations (Compton-regime approximation, $\delta\phi \approx 0$) and transverse spatial variations ($\partial/\partial x = 0 = \partial/\partial y$). Moreover, the analysis is carried out for the case of a finite-amplitude primary electromagnetic wave (ω_s, k_s) with right-circular polarization and vector potential specified by³⁷

$$\mathbf{A}_s(\mathbf{x}, t) = (mc^2/e)\hat{a}_s(z, t)\{\cos[k_s z - \omega_s t + \delta_s(z, t)]\hat{\mathbf{e}}_x - \sin[k_s z - \omega_s t + \delta_s(z, t)]\hat{\mathbf{e}}_y\}, \quad (2)$$

where the normalized amplitude $\hat{a}_s(z, t)$ and wave phase $\delta_s(z, t)$ are treated as slowly varying (Eikonal approximation). Here, $-e$ is the electron charge, m is the electron rest mass, and c is the speed of light *in vacuo*. In Eqs. (1) and (2), the wiggler magnetic field is determined from $\mathbf{B}_w = \nabla \times \mathbf{A}_w$, and the electromagnetic wave field is determined from $\mathbf{B}_s = \nabla \times \mathbf{A}_s$ and $\mathbf{E}_s = -c^{-1} \partial \mathbf{A}_s / \partial t$. A detailed investigation of the sideband instability simplifies considerably if the analysis is carried out in the ponderomotive frame moving with velocity^{37,71,72}

$$v_p = \omega_s / (k_s + k_0). \quad (3)$$

In the ponderomotive frame, it is found³⁷ that the transformed energy $\gamma'_j(t')$ is approximately constant, with $d\gamma'_j/dt' \approx 0$ in the Eikonal approximation [Eqs. (9) and

(14)]. This simplifies considerably the analytical treatment of the electron orbits in the combined helical wiggler field and the finite-amplitude primary electromagnetic wave. Therefore, the present analysis is carried out in ponderomotive-frame variables (z', t', γ') defined by the Lorentz transformation

$$\begin{aligned} z' &= \gamma_p(z - v_p t), \\ t' &= \gamma_p(t - v_p z/c^2), \\ \gamma' &= \gamma_p(\gamma - v_p p_z/mc^2), \end{aligned} \quad (4)$$

where $\gamma_p = (1 - v_p^2/c^2)^{-1/2}$, $\gamma' mc^2 = (m^2 c^4 + c^2 p_x'^2 + c^2 p_y'^2 + c^2 p_z'^2)^{1/2}$ is the mechanical energy, and the components of momentum (p_x', p_y', p_z') are related to the velocity $\mathbf{v}' = d\mathbf{x}'/dt'$ by $\mathbf{p}' = \gamma' m \mathbf{v}'$.

In the ponderomotive frame, the slow nonlinear evolution of $\hat{a}_s(z', t')$ and $\delta'_s(z', t')$ is described by³⁷

$$2\omega'_s \left(\frac{\partial}{\partial t'} + \frac{k'_s c^2}{\omega'_s} \frac{\partial}{\partial z'} \right) \hat{a}_s = \frac{4\pi e^2 a_w}{m} \frac{1}{L'} \left\langle \sum_j \frac{\sin(\theta'_{js} + \delta'_s)}{\gamma'_j} \right\rangle, \quad (5)$$

$$2\omega'_s \hat{a}_s \left(\frac{\partial}{\partial t'} + \frac{k'_s c^2}{\omega'_s} \frac{\partial}{\partial z'} \right) \delta'_s = \frac{4\pi e^2 a_w}{m} \frac{1}{L'} \left\langle \sum_j \frac{\cos(\theta'_{js} + \delta'_s)}{\gamma'_j} \right\rangle, \quad (6)$$

where the real oscillation frequency ω'_s and wavenumber k'_s are related by the dispersion relation³⁷

$$\omega_s'^2 = c^2 k_s'^2 + \frac{4\pi e^2}{m} \frac{1}{L'} \left\langle \sum_j \frac{1}{\gamma'_j} \right\rangle. \quad (7)$$

In Eqs. (5)–(7), $\langle \Sigma_j \dots \rangle$ denotes a statistical average, and the axial orbit $\theta'_{js}(t') = k'_p z'_j(t')$ and energy $\gamma'_j(t')$ of the j th electron solve³⁷

$$\begin{aligned} \frac{d^2}{dt'^2} \theta'_{js} + \frac{c^2 k_p'^2 a_w}{\gamma_j'^2} \text{Im}[\hat{a}_s \exp(i\theta'_{js} + i\delta'_s)] \\ = \frac{c^2 k_p' a_w}{\gamma_j'^2} \text{Re} \left[\exp(i\theta'_{js}) \left(\frac{\partial}{\partial z'_j} + \frac{1}{c^2} \frac{dz'_j}{dt'} \frac{\partial}{\partial t'} \right) \right. \\ \left. \times [\hat{a}_s \exp(i\delta'_s)] \right], \end{aligned} \quad (8)$$

and

$$\frac{d}{dt'} \gamma'_j = -\frac{a_w}{\gamma'_j} \text{Re} \left(\frac{\partial}{\partial t'} [\hat{a}_s \exp(i\delta'_s)] \right). \quad (9)$$

In Eqs. (8) and (9), $k_p' = (k_s + k_0)/\gamma_p$ is the wavenumber of the ponderomotive potential, and γ'_j is defined by

$$\begin{aligned} \gamma_j'^2 &= 1 + (p_{xj}'^2/m^2 c^2) + a_w^2 + \hat{a}_s^2 \\ &\quad - 2a_w \text{Re}[\hat{a}_s \exp(i\theta'_{js} + i\delta'_s)] \end{aligned} \quad (10)$$

in the ponderomotive frame. In obtaining Eqs. (8) and (9) from $dp'_{xj}/dt' = -mc^2 \partial \gamma'_j / \partial z'_j$ and $d\gamma'_j/dt' = \partial \gamma'_j / \partial t'$, we have neglected $\hat{a}_s^2 \ll 1 + a_w^2$ in Eq. (10). Moreover, it is assumed that all electrons have zero transverse canonical momentum, i.e., $P'_{xj} = 0 = P'_{yj}$.

There is some latitude in specifying the precise oper-

ational meaning³⁶ of the statistical averages $\langle \Sigma_j \dots \rangle$ occurring in Eqs. (5)–(7). For present purposes, let us assume that the orbits $z'_j(t')$ and $\gamma'_j(t')$ have been calculated from Eqs. (8) and (9) in terms of the initial values $z'_j(0)$ and $\gamma'_j(0)$. Then the simplest definition of the statistical average $\langle \Sigma_j \dots \rangle$ over some phase function $\psi(\theta'_{js}(0), \gamma'_j(0))$ is given by

$$\begin{aligned} \frac{1}{L'} \left\langle \sum_j \psi(\theta'_{js}(0), \gamma'_j(0)) \right\rangle \\ = \hat{n}'_b \int_0^{2\pi} \frac{d\theta'_0}{2\pi} \int_1^\infty d\gamma'_0 G(\theta'_0, \gamma'_0) \psi(\theta'_0, \gamma'_0). \end{aligned} \quad (11)$$

Here, \hat{n}'_b is the average density of the beam electrons in the ponderomotive frame, and $G(\theta'_0, \gamma'_0)$ is the (probability) distribution of electrons in initial phase θ'_0 and energy γ'_0 . Moreover, $L' = 2\pi/k'_p$ is the basic periodicity length in the ponderomotive frame.

Equations (5)–(9) constitute a closed description of the nonlinear evolution of the system. In this regard, further simplification of Eqs. (8) and (9) is possible by virtue of the assumption of slowly varying wave amplitude and phase (Eikonal approximation), i.e.,

$$\begin{aligned} |\omega'_s| \gg \left| [\hat{a}_s \exp(i\delta'_s)]^{-1} \frac{\partial}{\partial t'} [\hat{a}_s \exp(i\delta'_s)] \right|, \\ |k'_s| \gg \left| [\hat{a}_s \exp(i\delta'_s)]^{-1} \frac{\partial}{\partial z'} [\hat{a}_s \exp(i\delta'_s)] \right|. \end{aligned} \quad (12)$$

In particular, to lowest order, it is valid to neglect the local temporal and spatial derivatives on the right-hand sides of Eqs. (8) and (9). This gives the approximate dynamical equations³⁷

$$\frac{d^2}{dt'^2} \theta'_{js} + \frac{c^2 k_p'^2 a_w}{\gamma_j'^2} \text{Im}[\hat{a}_s \exp(i\theta'_{js} + i\delta'_s)] = 0, \quad (13)$$

$$\frac{d}{dt'} \gamma'_j = 0. \quad (14)$$

The major benefit of carrying out the analysis in the ponderomotive frame is evident from Eqs. (13) and (14). To lowest order, the particle energy γ'_j can be treated as constant in Eqs. (5)–(7) and (13).

In the subsequent analysis, we make use of the closed description of the nonlinear evolution of the system provided by Eqs. (5)–(7) and Eqs. (13) and (14).

B. Definitions and notation

For future reference, in this section we establish the basic definitions and notation to be used in the stability analysis in Secs. III and IV.

The wave frequency and wavenumber (ω', k') in the ponderomotive frame are related to the wave frequency and wavenumber (ω, k) in the laboratory frame by

$$\begin{aligned} \omega' &= \gamma_p(\omega - kv_p), \\ k' &= \gamma_p(k - \omega v_p/c^2), \end{aligned} \quad (15)$$

where v_p is defined in Eq. (3) and $\gamma_p = (1 - v_p^2/c^2)^{-1/2}$. As a special case, we obtain $\omega'_s = \gamma_p(\omega_s - k_s v_p)$ from Eq. (15), which gives

$$\omega'_s = \gamma_p k_0 v_p. \quad (16)$$

In the present analysis, it is also assumed that the electron beam is sufficiently tenuous that beam dielectric effects can be neglected in the dispersion relation (7) (and its laboratory-frame analog). This gives the vacuum dispersion relation $\omega_s^2 = c^2 k_s'^2$, or equivalently $\omega_s^2 = c^2 k_s^2$, for the primary electromagnetic wave. Assuming a forward-moving electromagnetic wave, we solve the simultaneous resonance conditions

$$\begin{aligned} \omega_s &= +ck_s, \\ \omega_s &= (k_s + k_0)v_p, \end{aligned} \quad (17)$$

for ω_s and k_s . This readily gives the familiar results³⁷

$$\begin{aligned} \omega_s &= \gamma_p^2 (1 + v_p/c) k_0 v_p, \\ k_s &= \gamma_p^2 (1 + v_p/c) (v_p/c) k_0, \end{aligned} \quad (18)$$

where v_p is (nearly) synchronous with the average axial velocity v_b of the beam electrons. Moreover, from Eqs. (18), the ponderomotive wave number $k_p' = (k_s + k_0)/\gamma_p$ can be expressed as

$$k_p' = \gamma_p (1 + v_p/c) k_0. \quad (19)$$

In circumstances where perturbations are about a primary electromagnetic wave with amplitude $\hat{a}_s^0 = \text{const}$ (independent of z' and t'), it is useful in analyzing the orbit equation (13) to introduce the bounce frequency $\hat{\omega}_B(\gamma_j')$ defined by²³

$$\hat{\omega}_B(\gamma_j') = (c^2 k_p'^2 a_w \hat{a}_s^0 / \gamma_j'^2)^{1/2}. \quad (20)$$

Here, $a_w > 0$ and $\hat{a}_s^0 > 0$ are assumed without loss of generality, and $\hat{\omega}_B(\gamma_j')$ is the effective bounce frequency of deeply trapped electrons with energy γ_j' . A detailed analysis²³ of Eqs. (10) and (13) shows that the zero-order electron motion is *untrapped* for energies γ_j' satisfying (Figs. 1 and 2)

$$\gamma_j' > \hat{\gamma}'_+ \equiv [1 + (a_w + \hat{a}_s^0)^2]^{1/2}. \quad (21)$$

That is, when Eq. (21) is satisfied, the particle motion is modulated by the ponderomotive potential, but the normalized velocity $d\theta_p^0/dt'$ does not change polarity (Fig. 1). On the other hand, for $\gamma_j' < \hat{\gamma}'_+$, the electrons are *trapped*, and the zero-order motion described by Eq. (13) is cyclic, corresponding to periodic motion in the ponderomotive potential. From Eqs. (10) and (13), it is readily shown that the minimum allowable energy of a trapped electron is²³

$$\hat{\gamma}'_- \equiv [1 + (a_w - \hat{a}_s^0)^2]^{1/2}. \quad (22)$$

Because $\hat{a}_s^0 \ll a_w$ in the regimes of practical interest, we note

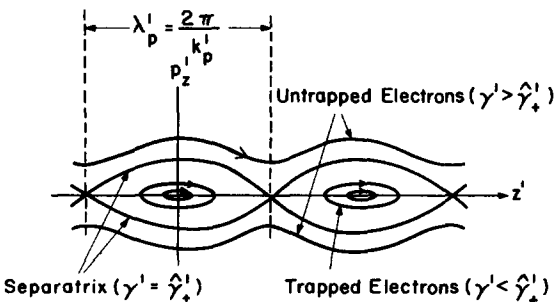


FIG. 1. In the ponderomotive frame, electron motion in the phase space (z', p_z') occurs on surfaces with $\gamma' = \text{const}$.

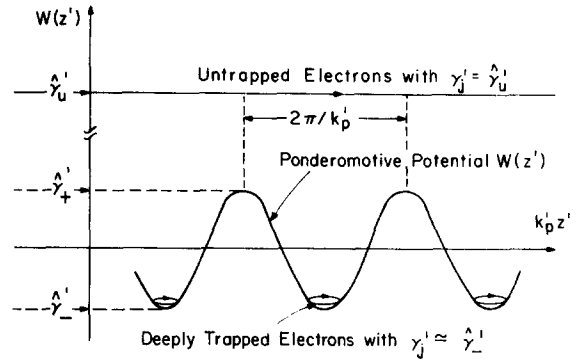


FIG. 2. Plot of the equilibrium ponderomotive potential $W(z') = \{\hat{\gamma}'^2 + 4a_w \hat{a}_s^0 \sin^2[\frac{1}{2}(k_p' z' + \delta_s^0)]\}^{1/2}$ vs $k_p' z'$. Here, $W(z')$ is the envelope of turning points with $p_z' = 0$ and $(\hat{a}_s, \delta_s^0) = (\hat{a}_s^0, \delta_s^0)$ in Eq. (10). Deeply trapped electrons have energy $\gamma_j' = \hat{\gamma}'_- = [1 + (a_w - \hat{a}_s^0)^2]^{1/2}$ [Eq. (22)]. Untrapped electrons have energy $\gamma_j' = \hat{\gamma}'_+ > \hat{\gamma}'_- = [1 + (a_w + \hat{a}_s^0)^2]^{1/2}$ [Eq. (21)]. Note that $\hat{\gamma}'_+ - \hat{\gamma}'_- = 4a_w \hat{a}_s^0 \ll 1$.

from Eqs. (21) and (22) that the characteristic energy of a trapped electron is approximately $\hat{\gamma}' \equiv (1 + a_w^2)^{1/2}$.

The stability analysis in Secs. III and IV specializes to the case where there are two classes of electrons: untrapped electrons with energy $\gamma_j' = \hat{\gamma}'_+ > \hat{\gamma}'_+$, and deeply trapped electrons with energy $\gamma_j' = \hat{\gamma}'_- \approx \hat{\gamma}'_-$. For the deeply trapped electrons, the effective bounce frequency in the laboratory frame is defined by $\Omega_B = \hat{\omega}_B(\hat{\gamma}'_-)/\gamma_p$, i.e.,

$$\Omega_B = (c^2 k_p'^2 a_w \hat{a}_s^0 / \gamma_p^2 \hat{\gamma}'_-^2)^{-1/2}. \quad (23)$$

Because $\hat{a}_s^0 \ll a_w$, we estimate $\hat{\gamma}'_- \approx \hat{\gamma}' \equiv (1 + a_w^2)^{1/2}$ in Eq. (23), and make use of Eq. (19) to express Eq. (23) in the equivalent (and more familiar) form

$$\Omega_B = \left(1 + \frac{v_p}{c}\right) \left(\frac{a_w \hat{a}_s^0}{1 + a_w^2}\right)^{1/2} ck_0. \quad (24)$$

Continuing with definitions, we denote the average density of the trapped electrons in the ponderomotive frame by $\hat{n}_T = \hat{n}_T/\gamma_p$, and the average density of the untrapped electrons by $\hat{n}_u = \hat{n}_u/\gamma_p$. It is convenient to introduce the corresponding plasma frequencies defined by

$$\begin{aligned} \hat{\omega}_{pT}^2 &= 4\pi \hat{n}_T e^2 / m = 4\pi \hat{n}_T e^2 / \gamma_p m, \\ \hat{\omega}_{pu}^2 &= 4\pi \hat{n}_u e^2 / m = 4\pi \hat{n}_u e^2 / \gamma_p m. \end{aligned} \quad (25)$$

A detailed investigation of Eqs. (5) and (6) (Secs. III and IV) shows that the appropriate small parameters, $\epsilon_T' \ll 1$ and $\epsilon_u' \ll 1$, used in analyzing the wave equations are defined by

$$\begin{aligned} \epsilon_T' ck_p' &= a_w \hat{\omega}_{pT}^2 / 2\omega_s' \hat{\gamma}'_- \hat{a}_s^0, \\ \epsilon_u' ck_p' &= a_w \hat{\omega}_{pu}^2 / 2\omega_s' \hat{\gamma}'_+ \hat{a}_s^0. \end{aligned} \quad (26)$$

Here, ω_s' is defined in Eq. (16), $\hat{\gamma}'_+$ is the energy of the untrapped electrons, and $\hat{\gamma}'_-$, $\hat{\omega}_{pT}^2$, and $\hat{\omega}_{pu}^2$ are defined in Eqs. (22) and (25). Note from Eqs. (25) and (26) that ϵ_T' and ϵ_u' are related by $\epsilon_T' = (\hat{n}_T/\hat{n}_u)(\hat{\gamma}'_+/\hat{\gamma}'_-)\epsilon_u'$. In Sec. III, we will find that ϵ_T' is related to the (slow) variation of the equilibrium wave phase δ_s^0 by $\partial\delta_s^0/\partial z' = \epsilon_T' ck_p'$ [Eq. (41)].

Finally, for future reference, we introduce the small dimensionless parameter Γ_T^3 defined by^{23,37}

$$\Gamma_T^3 = \frac{1}{4} \frac{a_w^2}{\hat{\gamma}'_-^3} \frac{\hat{\omega}_{pT}^2}{\gamma_p^2 c^2 k_0^2} \frac{(1 + v_p/c)}{v_p/c} \ll 1. \quad (27)$$

In the absence of untrapped electrons ($\hat{n}'_u = 0$), the quantity (3)^{1/2} $\Gamma_T c k_0/2$ can be identified with the linear gain (temporal growth rate) in the weak-pump regime ($\Omega_B/\Gamma_T c k_0 \ll 1$).³⁷ Moreover, from Eqs. (19), (23), (26), and (27), it can be shown that Γ_T and ϵ'_T are related by

$$\epsilon'_T = 2\Gamma_T (\Gamma_T c k_0/\Omega_B)^2. \quad (28)$$

From Eq. (28), we note that $\epsilon'_T \ll 1$ necessarily requires that the zero-order wave amplitude \hat{a}_s^0 be sufficiently large that $(\Omega_B/\Gamma_T c k_0)^2 \gg 2\Gamma_T$ (a small parameter).

III. STABILITY ANALYSIS FOR SMALL-AMPLITUDE PERTURBATIONS

A. Assumptions and model

We now make use of Eqs. (5), (6), and (13) with $\gamma'_j = \text{const}$ [Eq. (14)] to investigate detailed stability properties for small-amplitude perturbations about a quasisteady equilibrium state. The principal assumptions in the present analysis are the following.

(a) All of the trapped electrons are *deeply* trapped with a sharply defined energy $\gamma'_j = \hat{\gamma}'_T \approx \hat{\gamma}'_- = [1 + (a_w - \hat{a}_s^0)^2]^{1/2}$. From Eq. (13), this implies that the trapped electrons are spatially localized (“bunched”) near the bottom of the ponderomotive potential with $\theta'_{js} + \delta'_s \approx 2n\pi$, where $n = 0, \pm 1, \pm 2, \dots$ is an integer. The average density of the trapped electrons in the ponderomotive frame is $\hat{n}'_T = \hat{n}_T/\gamma_p$.

(b) All of the untrapped electrons have a sharply defined energy $\gamma'_j = \hat{\gamma}'_u > \hat{\gamma}'_+ = [1 + (a_w + \hat{a}_s^0)^2]^{1/2}$, where $\hat{\gamma}'_u$ is sufficiently large that the motion of the untrapped electrons is only weakly modulated by the ponderomotive potential. Strictly speaking, this requires that $\hat{\gamma}'_u^2 - \hat{\gamma}'_+^2$ be large in comparison with the total well depth $4a_w \hat{a}_s^0$.

(c) Consistent with (a) and (b), we assume that the perturbations are about a quasisteady equilibrium state characterized by $\hat{a}_s^0 = \text{const}$ (independent of z' and t') and $\partial \delta'_s/\partial t' = 0$. However, a slow spatial variation of the equilibrium phase δ'_s is required [Eq. (41)].^{37,71}

In the subsequent analysis, we denote the axial coordinate of the (deeply) trapped electrons with energy $\hat{\gamma}'_T \approx \hat{\gamma}'_-$ by $\theta'_T = k'_p z'_T(t')$, and the axial coordinate of the untrapped electrons with energy $\hat{\gamma}'_u$ is denoted by $\theta'_u = k'_p z'_u(t')$. The corresponding bounce frequencies are defined by

$$\begin{aligned} \hat{\omega}_{BT} &\equiv \hat{\omega}_B(\hat{\gamma}'_-) = (c^2 k_p'^2 a_w \hat{a}_s^0 / \hat{\gamma}'_-^2)^{1/2}, \\ \hat{\omega}_{Bu} &\equiv \hat{\omega}_B(\hat{\gamma}'_u) = (c^2 k_p'^2 a_w \hat{a}_s^0 / \hat{\gamma}'_u^2)^{1/2}, \end{aligned} \quad (29)$$

where $\hat{a}_s^0 = \text{const}$ is the equilibrium amplitude of the primary electromagnetic wave. Note from Eqs. (29) that $\hat{\omega}_{Bu} = (\hat{\gamma}'_-/\hat{\gamma}'_u) \hat{\omega}_{BT} \approx \hat{\omega}_{BT}$ because $\hat{\gamma}'_u$ typically exceeds $\hat{\gamma}'_-$ by only a small amount for $a_w \hat{a}_s^0 \ll 1$. Making use of assumptions (a)–(c), it readily follows from Eqs. (5), (6), and (13) that the nonlinear wave equations and the equations of motion for the trapped and untrapped electrons can be expressed as

$$\begin{aligned} \left(\frac{\partial}{\partial t'} + \frac{c^2 k'_s}{\omega'_s} \frac{\partial}{\partial z'} \right) \hat{a}_s &= \frac{a_w \hat{\omega}_{pT}^2}{2\omega'_s \hat{\gamma}'_-} \sin(\theta'_T + \delta'_s) \\ &+ \frac{a_w \hat{\omega}_{pu}^2}{2\omega'_s \hat{\gamma}'_u} \langle \sin(\theta'_u + \delta'_s) \rangle_u, \end{aligned} \quad (30)$$

$$\begin{aligned} \hat{a}_s \left(\frac{\partial}{\partial t'} + \frac{c^2 k'_s}{\omega'_s} \frac{\partial}{\partial z'} \right) \delta'_s &= \frac{a_w \hat{\omega}_{pT}^2}{2\omega'_s \hat{\gamma}'_-} \cos(\theta'_T + \delta'_s) \\ &+ \frac{a_w \hat{\omega}_{pu}^2}{2\omega'_s \hat{\gamma}'_u} \langle \cos(\theta'_u + \delta'_s) \rangle_u, \end{aligned} \quad (31)$$

and

$$\frac{d^2}{dt'^2} \theta'_T + \hat{\omega}_{BT}^2 \frac{\hat{a}_s}{\hat{a}_s^0} \sin(\theta'_T + \delta'_s) = 0, \quad (32)$$

$$\frac{d^2}{dt'^2} \theta'_u + \hat{\omega}_{Bu}^2 \frac{\hat{a}_s}{\hat{a}_s^0} \sin(\theta'_u + \delta'_s) = 0. \quad (33)$$

In Eqs. (30) and (31), $\hat{\omega}_{pT}^2$ and $\hat{\omega}_{pu}^2$ are defined in Eq. (25), and the statistical average $\langle \dots \rangle_u$ denotes an average over initial phases of the untrapped electrons, i.e.,

$$\langle \dots \rangle_u \equiv \int_0^{2\pi} \frac{d\theta'_u(0)}{2\pi} \dots \quad (34)$$

In terms of the small parameters ϵ'_T and ϵ'_u defined in Eq. (26), the nonlinear wave equations (30) and (31) can be expressed in the equivalent forms

$$\begin{aligned} \left(\frac{\partial}{\partial t'} + \frac{c^2 k'_s}{\omega'_s} \frac{\partial}{\partial z'} \right) \hat{a}_s &= \epsilon'_T c k'_p \hat{a}_s^0 \sin(\theta'_T + \delta'_s) \\ &+ \epsilon'_u c k'_p \hat{a}_s^0 \langle \sin(\theta'_u + \delta'_s) \rangle_u \end{aligned} \quad (35)$$

and

$$\begin{aligned} \hat{a}_s \left(\frac{\partial}{\partial t'} + \frac{c^2 k'_s}{\omega'_s} \frac{\partial}{\partial z'} \right) \delta'_s &= \epsilon'_T c k'_p \hat{a}_s^0 \cos(\theta'_T + \delta'_s) \\ &+ \epsilon'_u c k'_p \hat{a}_s^0 \langle \cos(\theta'_u + \delta'_s) \rangle_u. \end{aligned} \quad (36)$$

The coupled equations (32), (33), (35), and (36) constitute a closed description of the nonlinear evolution of the system within the context of assumptions (a)–(c).

We now make use of Eqs. (32), (33), (35), and (36) to investigate detailed properties of the sideband instability (including the influence of both trapped and untrapped electrons) for small-amplitude perturbations about a primary electromagnetic wave with constant amplitude \hat{a}_s^0 and slowly varying phase δ'_s . Each quantity is expressed as its equilibrium value plus a perturbation, i.e.,

$$\begin{aligned} \hat{a}_s &= \hat{a}_s^0 + \delta \hat{a}_s, & \delta'_s &= \delta'_s + \bar{\delta}'_s, \\ \theta'_T &= \theta'_T + \delta \theta'_T, & \theta'_u &= \theta'_u + \delta \theta'_u. \end{aligned} \quad (37)$$

For the deeply trapped electrons with $\theta'_T + \delta'_s \approx 2n\pi$, we take $n = 0$ without loss of generality in Eqs. (32), (35), and (36).

B. Equilibrium model

We first consider equilibrium solutions to Eqs. (32), (33), (35), and (36) in the absence of perturbations, i.e., $\delta\hat{a}_s = 0$, $\delta\tilde{s}' = 0$, $\delta\theta_T' = 0$, and $\delta\theta_u' = 0$. Consistent with the assumption that γ'_+ is sufficiently large in comparison with γ'_+ , the zero-order orbit of an untrapped electron calculated from Eq. (33) can be approximated by

$$\theta_u^0 = \theta_u^0(0) + \beta'_u c k'_p t'. \quad (38)$$

Here, $\beta'_u c = \text{const}$ is the average velocity of an untrapped electron in the ponderomotive frame. In Eq. (38), note that the modulation of the electron orbit by the ponderomotive potential has been neglected. Making use of Eq. (38) and the definition of the phase average in Eq. (34), it follows trivially that

$$\langle \sin(\theta_u^0 + \delta_s^0) \rangle_u = 0 = \langle \cos(\theta_u^0 + \delta_s^0) \rangle_u. \quad (39)$$

That is, in Eqs. (35) and (36), the untrapped electrons do not contribute to any change in the equilibrium amplitude \hat{a}_s^0 and phase δ_s^0 . Therefore, an appropriate quasisteady equilibrium state consistent with Eqs. (32), (35), and (36) is described by³⁷

$$\theta_T^0 + \delta_s^0 = 0, \quad (40a)$$

$$\frac{\partial}{\partial t'} \hat{a}_s^0 = 0 = \frac{\partial}{\partial z'} \hat{a}_s^0, \quad (40b)$$

and

$$\frac{\partial}{\partial t'} \delta_s^0 = 0, \quad (41a)$$

$$\frac{\partial}{\partial z'} \delta_s^0 = \epsilon'_T c k'_p. \quad (41b)$$

Note from Eqs. (41) that $\epsilon'_T \ll 1$ is required in the present analysis in order that the change in δ_s^0 be small over the scale length of the ponderomotive potential ($\lambda'_p = 2\pi k'_p{}^{-1}$). Making use of Eq. (28), the inequality $\epsilon'_T \ll 1$ is equivalent to $(\Omega_B/\Gamma_T c k_0)^2 \gg 2\Gamma_T$, where Γ_T is the small parameter defined in Eq. (27).

To summarize, the equilibrium state is characterized by free-streaming untrapped electrons [Eq. (38)], trapped electrons with $\theta_T^0 + \delta_s^0 = 0$ [Eq. (40a)], a primary electromagnetic wave with constant amplitude \hat{a}_s^0 [Eqs. (40)], and a slowly varying phase with $\partial\delta_s^0/\partial z' = \epsilon'_T c k'_p$ [Eq. (41b)].

C. Linearized equations

We now linearize Eqs. (32), (33), (35), and (37) for small-amplitude perturbations about the equilibrium state described by Eqs. (38)–(41). In this regard, it is convenient to introduce the normalized amplitude perturbation $\delta\hat{A}_s$, defined by

$$\delta\hat{A}_s = \delta\hat{a}_s/\hat{a}_s^0. \quad (42)$$

For $\theta_T' + \delta_s' \approx 0$, it is straightforward to show that the small-amplitude perturbations $\delta\theta_T'$, $\delta\theta_u'$, $\delta\hat{A}_s$, and $\delta\tilde{s}'$ evolve according to

$$\frac{d^2}{dt'^2} \delta\theta_T' + \hat{\omega}_{BT}^2 (\delta\theta_T' + \tilde{s}') = 0, \quad (43)$$

$$\begin{aligned} \frac{d^2}{dt'^2} \delta\theta_u' + \hat{\omega}_{Bu}^2 \cos(\theta_u^0 + \delta_s^0) \delta\theta_u' \\ = -\hat{\omega}_{Bu}^2 \text{Im} [(\delta\hat{A}_s + i\tilde{s}') \exp(i\theta_u^0 + i\delta_s^0)], \end{aligned} \quad (44)$$

$$\begin{aligned} \left(\frac{\partial}{\partial t'} + \frac{c^2 k'_s}{\omega'_s} \frac{\partial}{\partial z'} \right) \delta\hat{A}_s \\ = \epsilon'_T c k'_p (\delta\theta_T' + \tilde{s}') \\ + \epsilon'_u c k'_p \langle (\delta\theta_u' + \tilde{s}') \cos(\theta_u^0 + \delta_s^0) \rangle_u, \end{aligned} \quad (45)$$

$$\begin{aligned} \left(\frac{\partial}{\partial t'} + \frac{c^2 k'_s}{\omega'_s} \frac{\partial}{\partial z'} \right) \tilde{s}' + \epsilon'_T c k'_p \delta\hat{A}_s \\ = -\epsilon'_u c k'_p \langle (\delta\theta_u' + \tilde{s}') \sin(\theta_u^0 + \delta_s^0) \rangle_u. \end{aligned} \quad (46)$$

In Eqs. (43)–(46) it should be kept in mind that $\delta\hat{A}_s(z', t')$ and $\tilde{s}'(z', t')$ are real-valued functions. In analyzing Eqs. (43)–(46) it is useful to express

$$\delta\theta_u' = \delta\psi' \exp(i\theta_u^0 + i\delta_s^0) + \delta\psi'^* \exp(-i\theta_u^0 - i\delta_s^0), \quad (47)$$

where the complex amplitude $\delta\psi' = \delta\psi'_R + i\delta\psi'_I$ is slowly varying, and $\delta\psi'^*$ denotes the complex conjugate of $\delta\psi'$. Making use of Eqs. (44) and (47) and $\theta_u^0 = \theta_u^0(0) + \beta'_u c k'_p t'$, it is straightforward to show that $\delta\psi'$ evolves according to

$$\begin{aligned} \left(\frac{d^2}{dt'^2} + 2i\beta'_u c k'_p \frac{d}{dt'} \right. \\ \left. + [\hat{\omega}_{Bu}^2 \cos(\theta_u^0 + \delta_s^0) - \beta'^2_u c^2 k'^2_p] \right) \delta\psi' \\ = -(1/2i) \hat{\omega}_{Bu}^2 (\delta\hat{A}_s + i\tilde{s}'). \end{aligned} \quad (48)$$

For untrapped electron energy $\hat{\gamma}'_u$ sufficiently large in comparison with $\hat{\gamma}'_+ = [1 + (a_w + \hat{a}_s^0)^2]^{1/2}$, it is valid to neglect $\hat{\omega}_{Bu}^2 \cos(\theta_u^0 + \delta_s^0)$ in comparison with $\beta'^2_u c^2 k'^2_p$ in Eq. (48). Therefore, Eq. (48) can be approximated by

$$\begin{aligned} \left(\frac{d^2}{dt'^2} + 2i\beta'_u c k'_p \frac{d}{dt'} - \beta'^2_u c^2 k'^2_p \right) (\delta\psi'_R + i\delta\psi'_I) \\ = -(1/2i) \hat{\omega}_{Bu}^2 (\delta\hat{A}_s + i\tilde{s}'). \end{aligned} \quad (49)$$

In Eq. (49), $\delta\psi'_R$, $\delta\psi'_I$, $\delta\hat{A}_s$, and \tilde{s}' are all real quantities, and it follows that $\delta\psi'^* = \delta\psi'_R - i\delta\psi'_I$ evolves according to

$$\begin{aligned} \left(\frac{d^2}{dt'^2} - 2i\beta'_u c k'_p \frac{d}{dt'} - \beta'^2_u c^2 k'^2_p \right) (\delta\psi'_R - i\delta\psi'_I) \\ = (1/2i) \hat{\omega}_{Bu}^2 (\delta\hat{A}_s - i\tilde{s}'). \end{aligned} \quad (50)$$

Evidently, Eq. (49) [or Eq. (50)] describes the slow evolution of $\delta\psi'_R$ and $\delta\psi'_I$ in response to the amplifying wave perturbations $\delta\hat{A}_s$ and \tilde{s}' .

Substituting Eq. (47) into Eqs. (45) and (46), and making use of $\theta_u^0 = \theta_u^0(0) + \beta'_u c k'_p t'$ and the definition of the phase average in Eq. (34), it is straightforward to simplify the untrapped-electron contributions in the linearized wave equations. We readily obtain

$$\begin{aligned} \langle (\delta\theta_u' + \tilde{s}') \cos(\theta_u^0 + \delta_s^0) \rangle_u \\ = \langle \delta\theta_u' \cos(\theta_u^0 + \delta_s^0) \rangle_u = \delta\psi'_R, \end{aligned} \quad (51)$$

$$\begin{aligned} \langle (\delta\theta_u' + \tilde{s}') \sin(\theta_u^0 + \delta_s^0) \rangle_u \\ = \langle \delta\theta_u' \sin(\theta_u^0 + \delta_s^0) \rangle_u = -\delta\psi'_I. \end{aligned} \quad (52)$$

In Eqs. (51) and (52), the average of $\tilde{\delta}'_s$ times $\cos(\theta_u^0 + \delta_s^0)$ or $\sin(\theta_u^0 + \delta_s^0)$ vanishes because $\tilde{\delta}'_s$ is assumed to be slowly varying. Substituting Eqs. (51) and (52) into Eqs. (45) and (46), we obtain for the evolution of $\delta\hat{A}_s$ and $\tilde{\delta}'_s$

$$\left(\frac{\partial}{\partial t'} + \frac{c^2 k'_s}{\omega'_s} \frac{\partial}{\partial z'}\right) \delta\hat{A}_s = \epsilon'_T c k'_p (\delta\theta'_T + \tilde{\delta}'_s) + \epsilon'_u c k'_p \delta\psi'_R, \quad (53)$$

$$\left(\frac{\partial}{\partial t'} + \frac{c^2 k'_s}{\omega'_s} \frac{\partial}{\partial z'}\right) \tilde{\delta}'_s = -\epsilon'_T c k'_p \delta\hat{A}_s + \epsilon'_u c k'_p \delta\psi'_I. \quad (54)$$

To summarize, in the present analysis the final set of coupled, linearized equations for $\delta\theta'_T$, $\delta\psi'_R$, $\delta\psi'_I$, $\delta\hat{A}_s$, and $\tilde{\delta}'_s$ is given by Eqs. (43), (49), (50), (53), and (54).

D. Dispersion relation in ponderomotive frame

We now assume that the t' and z' dependence of the perturbations in Eqs. (43), (49), (50), (53), and (54) is proportional to

$$\exp[-i(\Delta\omega')t' + i(\Delta k')z'], \quad (55)$$

where $\text{Im}(\Delta\omega') > 0$ corresponds to instability (temporal growth). Consistent with neglecting beam dielectric effects in the dispersion relation (7), we also approximate $c^2 k'_s / \omega'_s = c$ in Eqs. (53) and (54). The linearized equations (43), (49), (50), (53), (54) then become

$$[(\Delta\omega')^2 - \hat{\omega}_{BT}^2] (\delta\theta'_T + \tilde{\delta}'_s) = (\Delta\omega')^2 \tilde{\delta}'_s, \quad (56)$$

$$-(\Delta\omega' - \beta'_u c k'_p)^2 (\delta\psi'_R + i\delta\psi'_I) = -(1/2i) \hat{\omega}_{Bu}^2 (\delta\hat{A}_s + i\tilde{\delta}'_s), \quad (57)$$

$$-(\Delta\omega' + \beta'_u c k'_p)^2 (\delta\psi'_R - i\delta\psi'_I) = (1/2i) \hat{\omega}_{Bu}^2 (\delta\hat{A}_s - i\tilde{\delta}'_s), \quad (58)$$

$$-i(\Delta\omega' - c\Delta k') \delta\hat{A}_s = \epsilon'_T c k'_p (\delta\theta'_T + \tilde{\delta}'_s) + \epsilon'_u c k'_p \delta\psi'_R, \quad (59)$$

$$-i(\Delta\omega' - c\Delta k') \tilde{\delta}'_s = -\epsilon'_T c k'_p \delta\hat{A}_s + \epsilon'_u c k'_p \delta\psi'_I. \quad (60)$$

In Eqs. (57) and (58), it is useful to introduce the untrapped-electron susceptibilities χ^+ and χ^- defined by

$$\chi^+(\Delta k', \Delta\omega') = \frac{\hat{\omega}_{Bu}^2}{(\Delta\omega' + \beta'_u c k'_p)^2} + \frac{\hat{\omega}_{Bu}^2}{(\Delta\omega' - \beta'_u c k'_p)^2}, \quad (61)$$

$$\chi^-(\Delta k', \Delta\omega') = \frac{\hat{\omega}_{Bu}^2}{(\Delta\omega' + \beta'_u c k'_p)^2} - \frac{\hat{\omega}_{Bu}^2}{(\Delta\omega' - \beta'_u c k'_p)^2}. \quad (62)$$

From Eqs. (57) and (58) we readily obtain

$$\delta\psi'_R = \frac{1}{4}(i\chi^- \delta\hat{A}_s + \chi^+ \tilde{\delta}'_s), \quad (63)$$

$$\delta\psi'_I = \frac{1}{4}(-\chi^+ \delta\hat{A}_s + i\chi^- \tilde{\delta}'_s), \quad (64)$$

which express $\delta\psi'_R$ and $\delta\psi'_I$ directly in terms of the perturbed amplitude $\delta\hat{A}_s$ and phase $\tilde{\delta}'_s$. Solving Eq. (56) for $\delta\theta'_T + \tilde{\delta}'_s$ in terms of $\tilde{\delta}'_s$ and substituting Eqs. (63) and (64) into Eqs. (59) and (60) give two coupled homogeneous equations for $\delta\hat{A}_s$ and $\tilde{\delta}'_s$. Setting the resulting two-by-two determinant equal to zero, we obtain, after some straightforward algebraic manipulation,

$$\begin{aligned} & [(\Delta\omega' - c\Delta k') + \frac{1}{4}\epsilon'_u c k'_p \chi^-]^2 \\ & = (\epsilon'_T c k'_p \{(\Delta\omega')^2 / [(\Delta\omega')^2 - \hat{\omega}_{BT}^2]\} + \frac{1}{4}\epsilon'_u c k'_p \chi^+) \\ & \quad \times (\epsilon'_T c k'_p + \frac{1}{4}\epsilon'_u c k'_p \chi^+). \end{aligned} \quad (65)$$

Equation (65) is the desired dispersion relation which relates the (complex) oscillation frequency $\Delta\omega'$ to the wave-number $\Delta k'$ and the system parameters ϵ'_T , ϵ'_u , $c k'_p$, etc. Here, ϵ'_T , ϵ'_u , χ^+ , and χ^- are defined in Eqs. (26), (61), and (62).

Before investigating detailed stability properties (Sec. IV), we show that the dispersion relation (65) reduces to familiar results in two limiting cases: (a) no untrapped electrons ($\hat{n}'_u = 0$), and (b) no trapped electrons ($\hat{n}'_T = 0$).

No untrapped electrons ($\hat{n}'_u = 0$): For $\hat{n}'_u = 0$, it follows from Eq. (26) that $\epsilon'_u = 0$, and Eq. (65) reduces to

$$(\Delta\omega' - c\Delta k')^2 = \epsilon'^2_T c^2 k_p'^2 [(\Delta\omega')^2 / (\Delta\omega')^2 - \hat{\omega}_{BT}^2]. \quad (66)$$

Equation (66) can be expressed in the equivalent form

$$0 = 1 - \frac{\hat{\omega}_{BT}^2}{(\Delta\omega')^2} - \frac{\epsilon'^2_T c^2 k_p'^2}{(\Delta\omega' - c\Delta k')^2}, \quad (67)$$

which is the familiar dispersion relation^{37,73} for the sideband instability assuming slowly varying equilibrium phase δ_s^0 and no untrapped electrons. The detailed stability properties predicted by Eq. (67) are investigated in Ref. 37.

No trapped electrons ($\hat{n}'_T = 0$): For $\hat{n}'_T = 0$, it follows from Eq. (26) that $\epsilon'_T = 0$, and Eq. (65) can be expressed as

$$\begin{aligned} 0 = & \{(\Delta\omega' - c\Delta k') - \frac{1}{2}\epsilon'_u c k'_p [\hat{\omega}_{Bu}^2 / (\Delta\omega' - \beta'_u c k'_p)^2]\} \\ & \times \{(\Delta\omega' - c\Delta k') + \frac{1}{2}\epsilon'_u c k'_p \\ & \times [\hat{\omega}_{Bu}^2 / (\Delta\omega' + \beta'_u c k'_p)^2]\}, \end{aligned} \quad (68)$$

where ϵ'_u and $\hat{\omega}_{Bu}^2$ are defined in Eqs. (26) and (29), and use has been made of Eqs. (61) and (62). Apart from a sign, the two factors in Eq. (68) are identical under the (simultaneous) reflections $\Delta\omega' \rightarrow -\Delta\omega'$ and $\Delta k' \rightarrow -\Delta k'$. Setting the first factor in Eq. (68) equal to zero gives the dispersion relation

$$(\Delta\omega' - c\Delta k') (\Delta\omega' - \beta'_u c k'_p)^2 = a_w^2 \hat{\omega}_{pu}^2 c^2 k_p'^2 / 4\hat{\gamma}_u'^3 \omega'_s, \quad (69)$$

where use has been made of Eqs. (26) and (29). Consistent with assumption (b), we note that Eq. (69) is independent of the equilibrium wave amplitude \hat{a}_s^0 . When $\Delta\omega'$ and $\Delta k'$ are transformed back to the laboratory frame, it is straightforward to show that Eq. (69) is similar to the Compton-regime dispersion relation⁶⁶ obtained in the small-signal limit in the absence of trapped electrons.

We now return to the full dispersion relation in Eq. (65).

Alternate form of the full dispersion relation: It is useful to rewrite Eq. (65) in an alternate form which clearly delineates the trapped- and untrapped-electron contributions. Making use of Eqs. (61) and (62), rearranging terms in Eq. (65), and multiplying Eq. (65) by $[(\Delta\omega')^2 - \hat{\omega}_{BT}^2] / (\Delta\omega')^2 \times (\Delta\omega' - c\Delta k')^2$, it is straightforward to show that the dispersion relation can be expressed in the equivalent form

$$1 - \frac{\hat{\omega}_{BT}^2}{(\Delta\omega')^2} - \frac{\epsilon_T'^2 c^2 k_p'^2}{(\Delta\omega' - c\Delta k')^2} = \frac{1}{2} \epsilon_u' c k_p' \hat{\omega}_{Bu}^2 \frac{[(\Delta\omega')^2 - \hat{\omega}_{BT}^2]}{(\Delta\omega')^2 (\Delta\omega' - c\Delta k')^2 [(\Delta\omega')^2 - \beta_u'^2 c^2 k_p'^2]} \times \left[\frac{1}{2} \epsilon_u' c k_p' \hat{\omega}_{Bu}^2 + 4\Delta\omega' (\Delta\omega' - c\Delta k') \beta_u' c k_p' + \epsilon_T' c k_p' [(\Delta\omega')^2 + \beta_u'^2 c^2 k_p'^2] \left(1 + \frac{(\Delta\omega')^2}{(\Delta\omega')^2 - \hat{\omega}_{BT}^2} \right) \right]. \quad (70)$$

Here, ϵ_T' , ϵ_u' , $\hat{\omega}_{BT}$, and $\hat{\omega}_{Bu}$ are defined in Eqs. (26) and (29). In the absence of untrapped electrons ($\epsilon_u' = 0$), we note that Eq. (70) reduces directly to the familiar dispersion relation (67) for the sideband instability. That is, the effects of the untrapped electrons (the terms proportional to ϵ_u') are incorporated on the right-hand side of Eq. (70).

IV. ANALYSIS OF DISPERSION RELATION

A. Dispersion relation in laboratory frame

We now transform the full dispersion relation (70) back to the laboratory frame. From Eq. (15), it follows that

$$\begin{aligned} \Delta\omega' &= \gamma_p (\Delta\omega - v_p \Delta k), \\ \Delta k' &= \gamma_p [\Delta k - (v_p/c^2) \Delta\omega], \end{aligned} \quad (71)$$

where $\Delta\omega$ and Δk are the frequency and wavenumber of the perturbations in the laboratory frame. Making use of Eq. (71) and $\gamma_p^2 = (1 - v_p^2/c^2)^{-1}$, it is straightforward to show that³⁷

$$\Delta\omega' - c\Delta k' = \gamma_p \left(1 + \frac{v_p}{c} \right) \left(\Delta\omega - v_p \Delta k - c k_0 \frac{v_p}{c} \frac{\Delta k}{k_s} \right), \quad (72)$$

where k_s is defined in Eq. (18). We further introduce the shorthand notation

$$\Delta\Omega = \Delta\omega - v_p \Delta k, \quad (73a)$$

$$\Delta K = k_0 (v_p/c) (\Delta k/k_s). \quad (73b)$$

Then, from Eqs. (71)–(73), $\Delta\omega'$ and $\Delta\omega' - c\Delta k'$ can be expressed in the equivalent form

$$\Delta\omega' = \gamma_p \Delta\Omega, \quad (74a)$$

$$\Delta\omega' - c\Delta k' = \gamma_p (1 + v_p/c) (\Delta\Omega - c\Delta K). \quad (74b)$$

Equations (74) express $\Delta\omega'$ and $\Delta\omega' - c\Delta k'$ directly in terms of $\Delta\Omega$ and ΔK , which are related to $\Delta\omega$ and Δk in the laboratory frame by Eqs. (73).

To simplify the dispersion relation (70), it is convenient to introduce the dimensionless parameter

$$\alpha_u = (\hat{n}'_u/\hat{n}'_T) (\hat{\gamma}'_-/\hat{\gamma}'_u)^3, \quad (75)$$

which is a measure of the ratio of the untrapped-electron density to the trapped-electron density, $\hat{n}'_u/\hat{n}'_T = \hat{n}_u/\hat{n}_T$. Making use of Eqs. (16), (19), (25), (26), (28), (29), and (75), some straightforward algebra shows that $\epsilon_T' c k_p'$ and $\epsilon_u' c k_p' \hat{\omega}_{Bu}^2$ can be expressed in the equivalent forms

$$\epsilon_T' c k_p' = 2\Gamma_T c k_0 (\Gamma_T c k_0/\Omega_B)^2 \gamma_p (1 + v_p/c) \quad (76)$$

and

$$\epsilon_u' c k_p' \hat{\omega}_{Bu}^2 = 2\alpha_u (\Gamma_T c k_0)^3 \gamma_p^3 (1 + v_p/c). \quad (77)$$

Here, Γ_T is the (small) dimensionless gain parameter de-

defined in Eq. (27), and the bounce frequency $\Omega_B = (c^2 k_p'^2 a_w \times \hat{a}_s^0/\hat{\gamma}'_- \gamma_p^2)^{1/2}$ of the deeply trapped electrons is defined in the laboratory frame in Eqs. (23) and (24). Finally, making use of Eq. (19), we note that $\beta_u' c k_p' = \gamma_p (1 + v_p/c) \beta_u' c k_0$. It is useful to define

$$\hat{\beta}'_u = (1 + v_p/c) \beta'_u \quad (78)$$

so that $\beta_u' c k_p'$ can be expressed in the compact form

$$\beta_u' c k_p' = \gamma_p \hat{\beta}'_u c k_0. \quad (79)$$

After some algebraic manipulation that makes use of $\Omega_B = \hat{\omega}_{BT}/\gamma_p$ and Eqs. (74), (76), (77), and (79), it is straightforward to show that the dispersion relation (70) can be expressed in the equivalent form

$$1 - \frac{\Omega_B^2}{(\Delta\Omega)^2} - \frac{4\Omega_B^2 (\Gamma_T c k_0/\Omega_B)^6}{(\Delta\Omega - c\Delta K)^2} = \alpha_u \frac{(\Gamma_T c k_0)^3 [(\Delta\Omega)^2 - \Omega_B^2]}{(\Delta\Omega)^2 (\Delta\Omega - c\Delta K)^2 [(\Delta\Omega)^2 - \hat{\beta}'_u{}^2 c^2 k_0^2]} \times \left[\alpha_u (\Gamma_T c k_0)^3 + 4(\Delta\Omega) (\Delta\Omega - c\Delta K) \hat{\beta}'_u c k_0 + 2(\Gamma_T c k_0) \left(\frac{\Gamma_T c k_0}{\Omega_B} \right)^2 [(\Delta\Omega)^2 + \hat{\beta}'_u{}^2 c^2 k_0^2] \right] \times \left(1 + \frac{(\Delta\Omega)^2}{(\Delta\Omega)^2 - \Omega_B^2} \right). \quad (80)$$

Here, $\alpha_u = (\hat{n}'_u/\hat{n}'_T) (\hat{\gamma}'_-/\hat{\gamma}'_u)^3$ [Eq. (75)], $\Delta\Omega = \Delta\omega - v_p \Delta k$ [Eqs. (73)], $\Delta K = k_0 (v_p/c) \Delta k/k_s$ [Eqs. (73)], and Γ_T is the (small) dimensionless gain parameter defined in Eq. (27). For $a_w \hat{a}_s^0 \ll 1$, making use of Eq. (27), we find that Γ_T can also be expressed in the more familiar form

$$\Gamma_T^3 = \frac{1}{4} \frac{a_w^2}{(1 + a_w^2)^{3/2}} \frac{(4\pi \hat{n}_T e^2/m)}{\gamma_p^2 c^2 k_0^2} \frac{(1 + v_p/c)}{v_p/c} \ll 1, \quad (81)$$

where use has been made of $\hat{n}'_T = \hat{n}_T/\gamma_p$. Consistent with assumption (b) at the beginning of Sec. III, we require that $\hat{\beta}'_u c k_0$ be sufficiently large in comparison with Ω_B in Eq. (80) in order that the untrapped-electron motion be only weakly modulated by the ponderomotive potential.

Equation (80) constitutes the final dispersion relation analyzed numerically in Sec. IV B. For $\alpha_u = 0$, which corresponds to no untrapped electrons ($\hat{n}'_u = 0$), Eq. (80) is the familiar dispersion relation^{37,71} for the sideband instability in circumstances where the equilibrium wave phase is slowly varying [Eq. (41)]. For $\alpha_u \neq 0$, however, it is found that the untrapped electrons can significantly modify stability behavior (Sec. IV B).

B. Numerical results

In analyzing the dispersion relation (80) it is sensible to introduce the *total* density of beam electrons $\hat{n}_b = \hat{n}_T + \hat{n}_u$. We define the fraction of beam electrons that are untrapped (f_u) and the fraction of beam electrons that are trapped (f_T) by

$$\begin{aligned} f_u &= \hat{n}_u / \hat{n}_b, \\ f_T &= \hat{n}_T / \hat{n}_b = 1 - f_u. \end{aligned} \quad (82)$$

(Keep in mind that $\hat{n}'_u = \hat{n}_u / \gamma_p$, $\hat{n}'_T = \hat{n}_T / \gamma_p$, and $\hat{n}'_b = \hat{n}_b / \gamma_p$ are the densities in the ponderomotive frame. Therefore, f_u and f_T are also given by $f_u = \hat{n}'_u / \hat{n}'_b$ and $f_T = \hat{n}'_T / \hat{n}'_b$.) We further define the gain factor Γ_b associated with the total beam density by

$$\Gamma_b^3 = (\hat{n}_b / \hat{n}_T) \Gamma_T^3, \quad (83)$$

where Γ_T^3 is defined in Eq. (81). Because $(\hat{\gamma}'_- / \hat{\gamma}'_+)^3 \approx 1$ for $a_u \hat{a}_s^0 \ll 1$, it follows from Eq. (75) that $\alpha_u = \hat{n}'_u / \hat{n}'_T = \hat{n}_u / \hat{n}_T$ is an excellent approximation. Therefore, from Eqs. (82) and (83), $\alpha_u \Gamma_T^3$ and Γ_T^3 can be expressed in terms of Γ_b^3 and f_u by

$$\alpha_u \Gamma_T^3 = f_u \Gamma_b^3, \quad \Gamma_T^3 = (1 - f_u) \Gamma_b^3, \quad (84)$$

where $f_u = \hat{n}_u / \hat{n}_b$ is the fraction of beam electrons that are untrapped.

In the numerical analysis of Eq. (80), we normalize all frequencies to $\Gamma_b c k_0$ and introduce the dimensionless parameters

$$\begin{aligned} \Delta \tilde{\Omega} &= \Delta \tilde{\Omega} / \Gamma_b c k_0, \quad \Delta \tilde{K} = c \Delta K / \Gamma_b c k_0, \\ \tilde{\Omega}_B &= \Omega_B / \Gamma_b c k_0, \quad \tilde{\beta}_u = \hat{\beta}'_u c k_0 / \Gamma_b c k_0. \end{aligned} \quad (85)$$

In Eqs. (85) note that $\tilde{\Omega}_B = \Omega_B / \Gamma_b c k_0$ is a dimensionless measure of the pump strength (amplitude of the primary electromagnetic wave). In Eqs. (85) we have normalized all quantities to $\Gamma_b c k_0$, which (within a constant factor) is the usual FEL growth rate for a cold, unbunched, electron beam with density \hat{n}_b . Alternatively, quantities could have been normalized to the synchrotron frequency Ω_B . The latter normalization, however, would be less satisfactory because we wish to investigate detailed stability properties over a wide range of Ω_B and f_u (with \hat{n}_b fixed). Substituting Eqs. (84) and (85) into Eq. (80), we find that the dispersion relation can be expressed in the equivalent form

$$\begin{aligned} 1 - \frac{\tilde{\Omega}_B^2}{(\Delta \tilde{\Omega})^2} - \frac{4(1 - f_u)^2 \tilde{\Omega}_B^4}{(\Delta \tilde{\Omega} - \Delta \tilde{K})^2} \\ = \frac{f_u [(\Delta \tilde{\Omega})^2 - \tilde{\Omega}_B^2]}{(\Delta \tilde{\Omega})^2 (\Delta \tilde{\Omega} - \Delta \tilde{K})^2 [(\Delta \tilde{\Omega})^2 - \tilde{\beta}_u^2]^2} \\ \times \left[f_u + 4(\Delta \tilde{\Omega})(\Delta \tilde{\Omega} - \Delta \tilde{K}) \tilde{\beta}_u + \frac{2(1 - f_u)}{\tilde{\Omega}_B^2} \right. \\ \left. \times [(\Delta \tilde{\Omega})^2 + \tilde{\beta}_u^2] \left(1 + \frac{(\Delta \tilde{\Omega})^2}{(\Delta \tilde{\Omega})^2 - \tilde{\Omega}_B^2} \right) \right]. \end{aligned} \quad (86)$$

The dispersion relation (86) has been solved numerically for the normalized growth rate $\text{Im}(\Delta \tilde{\Omega})$

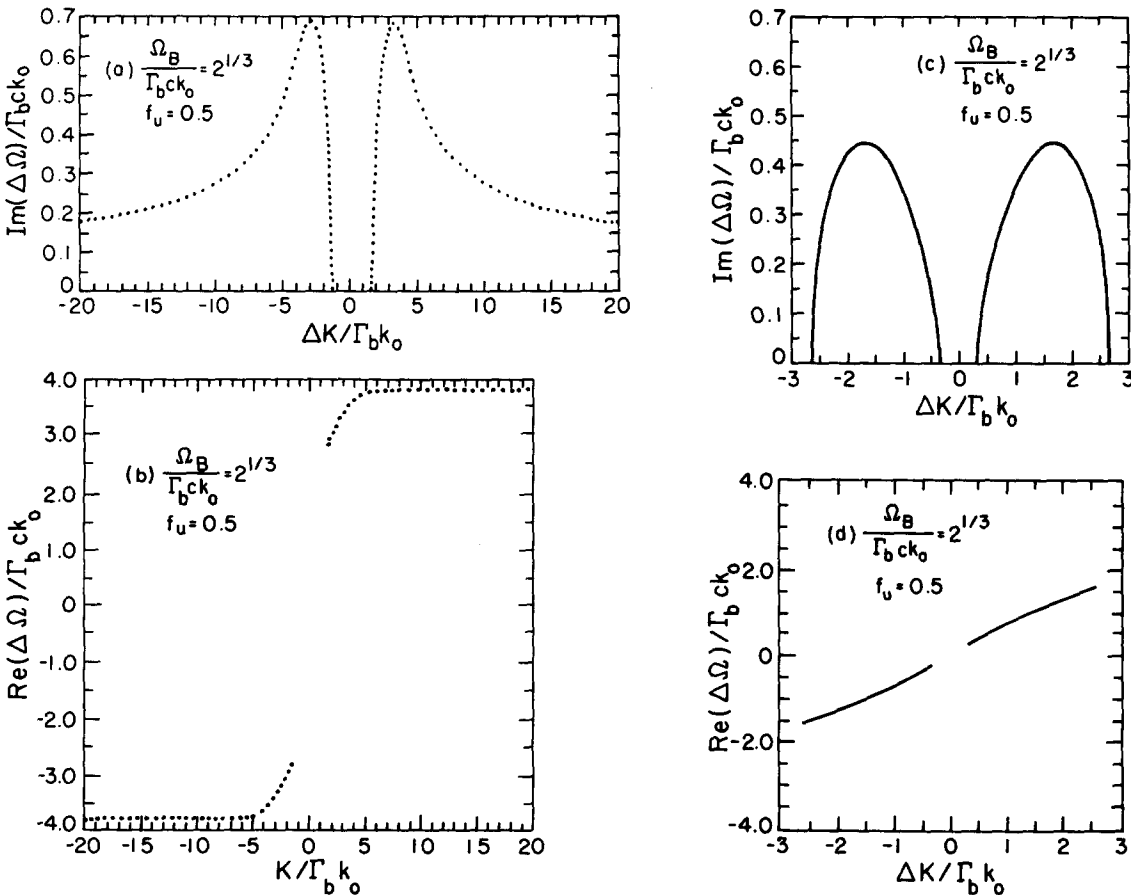


FIG. 3. Plots of the normalized growth rate $\text{Im}(\Delta \Omega) / \Gamma_b c k_0$ and real frequency $\text{Re}(\Delta \Omega) / \Gamma_b c k_0$ vs $\Delta K / \Gamma_b k_0$ obtained from Eq. (86) for the untrapped-electron mode [(a) and (b)] and the trapped-electron mode [(c) and (d)]. Results are presented for $\Omega_B / \Gamma_b c k_0 = 2^{1/3}$, $\tilde{\beta}_u = 3 \times 2^{1/3}$, and $f_u = 0.5$.

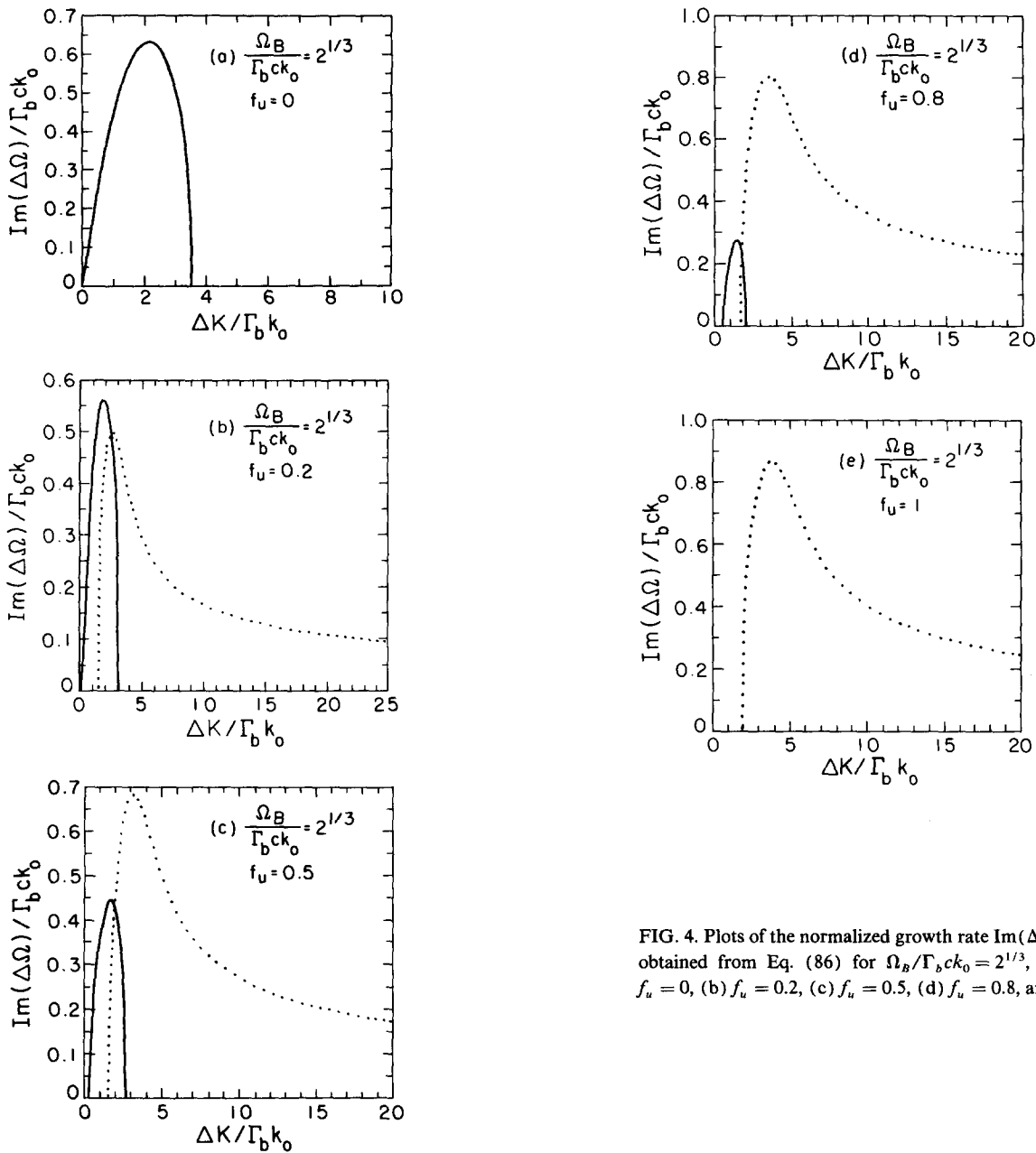


FIG. 4. Plots of the normalized growth rate $\text{Im}(\Delta\Omega)/\Gamma_b ck_0$ vs $\Delta K/\Gamma_b k_0$ obtained from Eq. (86) for $\Omega_B/\Gamma_b ck_0 = 2^{1/3}$, $\tilde{\beta}_u = 3 \times 2^{1/3}$, and (a) $f_u = 0$, (b) $f_u = 0.2$, (c) $f_u = 0.5$, (d) $f_u = 0.8$, and (e) $f_u = 1$.

$= \text{Im}(\Delta\Omega)/\Gamma_b ck_0$ and the normalized real frequency $\text{Re}(\Delta\tilde{\Omega}) = \text{Re}(\Delta\Omega)/\Gamma_b ck_0$ versus the normalized wavenumber $\tilde{\Delta K} = \Delta K/\Gamma_b k_0$ over a wide range of system parameters $\tilde{\Omega}_B = \Omega_B/\Gamma_b ck_0$, $f_u = \hat{n}_u/\hat{n}_b$, and $\tilde{\beta}_u = \tilde{\beta}'_u/\Gamma_b$. Typical results are illustrated in Figs. 3–8 for a fixed value of $\tilde{\beta}_u = 3 \times 2^{1/3} = 4.3267$, and normalized pump strength ranging from $\Omega_B/\Gamma_b ck_0 = 2^{1/3} = 1.2599$ (Figs. 3–5), to $\Omega_B/\Gamma_b ck_0 = 0.5$ (Fig. 6), to $\Omega_B/\Gamma_b ck_0 = 0.2$ (Figs. 7 and 8).

In Fig. 3, we illustrate typical numerical results and establish the sign conventions inherent in the dispersion relation (86). In particular, for $\Omega_B/\Gamma_b ck_0 = 2^{1/3}$ and $f_u = \hat{n}_u/\hat{n}_b = 0.5$, Fig. 3 shows plots of the normalized growth rate $\text{Im}(\Delta\Omega)/\Gamma_b ck_0$ and real oscillation frequency $\text{Re}(\Delta\Omega)/\Gamma_b ck_0$ versus normalized wavenumber $\Delta K/\Gamma_b k_0$ obtained from Eq. (86) for the two classes of unstable solutions. The results in Figs. 3(a) and 3(b) pertain to the unstable mode driven by the *untrapped electrons*, whereas the re-

sults in Figs. 3(c) and 3(d) pertain to the unstable mode driven by the *trapped electrons*. For $f_u = \hat{n}_u/\hat{n}_b = 0.5$, both classes of unstable modes are of course affected by the other population of electrons. With regard to the symmetries inherent in Eq. (86) and evident in Fig. 3, we note that

$$\begin{aligned} \text{Re } \Delta\Omega(-\Delta K) &= -\text{Re } \Delta\Omega(\Delta K), \\ \text{Im } \Delta\Omega(-\Delta K) &= \text{Im } \Delta\Omega(\Delta K), \end{aligned} \quad (87)$$

are (necessarily) satisfied by both classes of unstable modes. Equation (87) assures that the Fourier transform functions for the perturbed quantities $\delta \hat{A}_s, \delta \hat{\delta}_s, \delta \theta'_T$, etc., correspond to transforms of *real-valued* functions. The roots of Eq. (86) corresponding to the trapped-electron mode and the untrapped-electron mode are distinguished by tracking both $\text{Re}(\Delta\Omega)$ and $\text{Im}(\Delta\Omega)$ for the two modes; the real frequency shifts for these two modes are clearly separated, as is evident from Figs. 3(b) and 3(d). For simplicity of notation, keep-

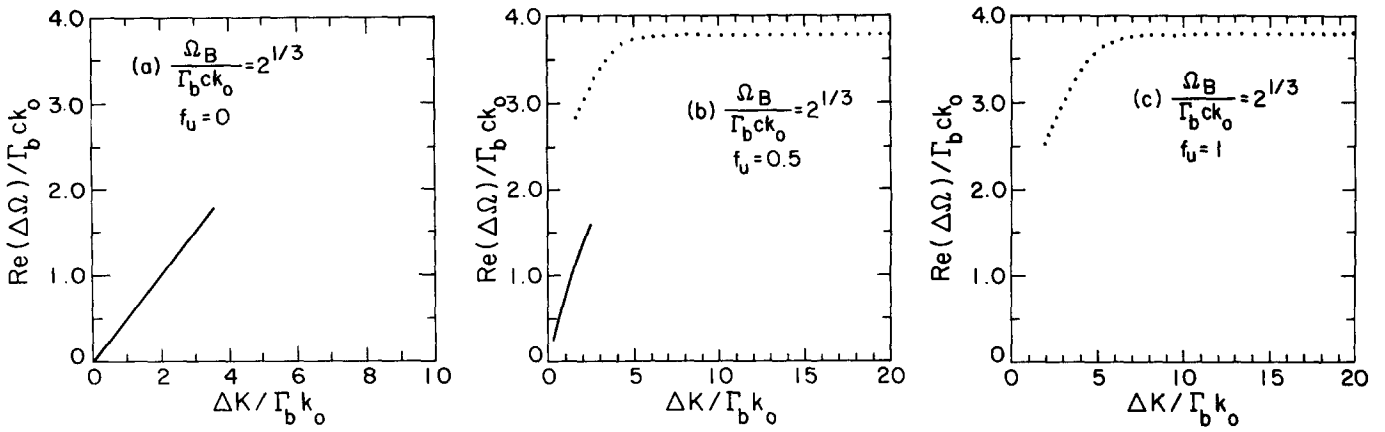


FIG. 5. Plots of the normalized real frequency $\text{Re}(\Delta\Omega)/\Gamma_b ck_0$ vs $\Delta K/\Gamma_b k_0$ obtained from Eq. (86) for $\Omega_B/\Gamma_b ck_0 = 2^{1/3}$, $\beta_u = 3 \times 2^{1/3}$, and (a) $f_u = 0$, (b) $f_u = 0.5$, and (c) $f_u = 1$.

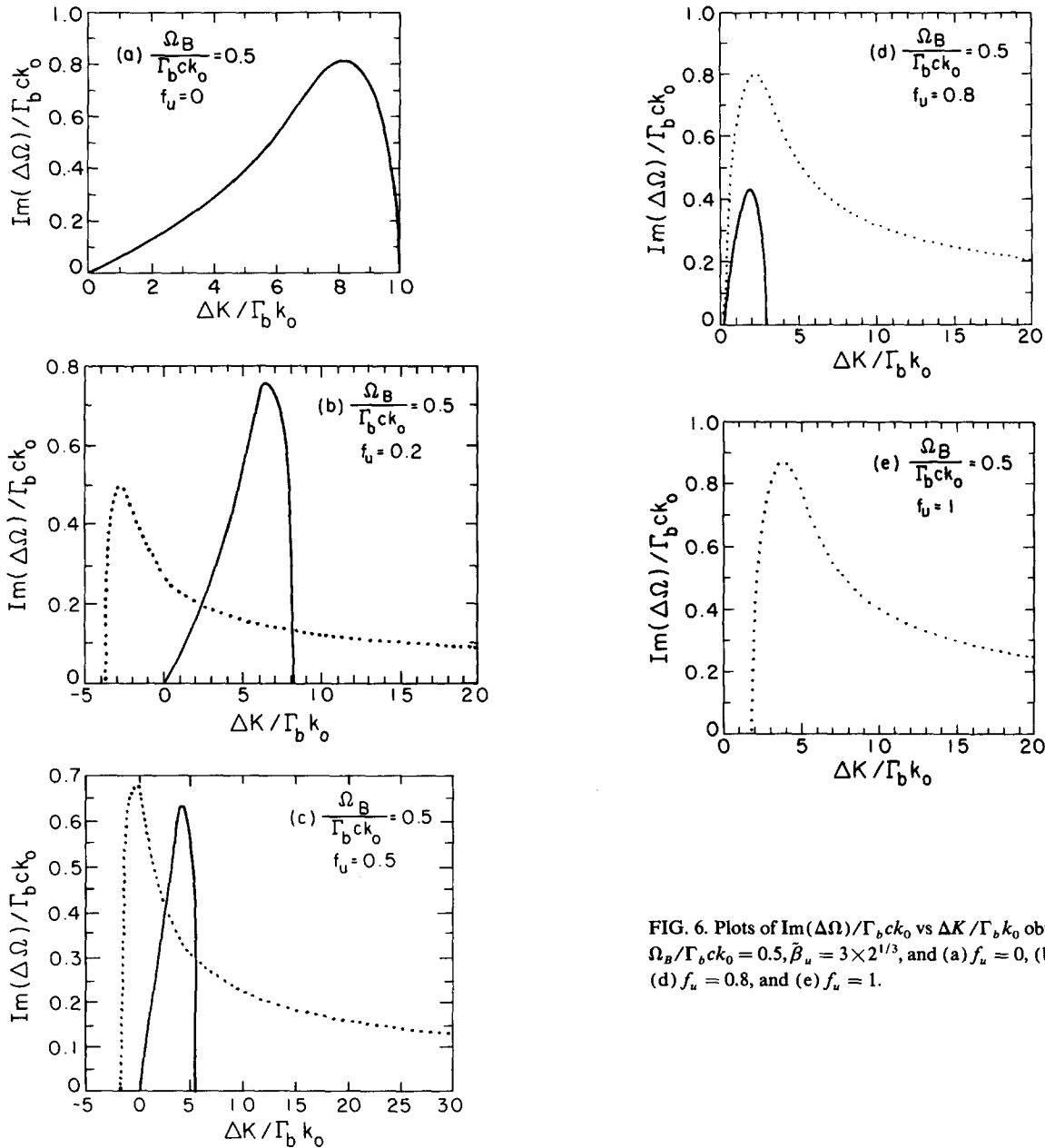


FIG. 6. Plots of $\text{Im}(\Delta\Omega)/\Gamma_b ck_0$ vs $\Delta K/\Gamma_b k_0$ obtained from Eq. (86) for $\Omega_B/\Gamma_b ck_0 = 0.5$, $\beta_u = 3 \times 2^{1/3}$, and (a) $f_u = 0$, (b) $f_u = 0.2$, (c) $f_u = 0.5$, (d) $f_u = 0.8$, and (e) $f_u = 1$.

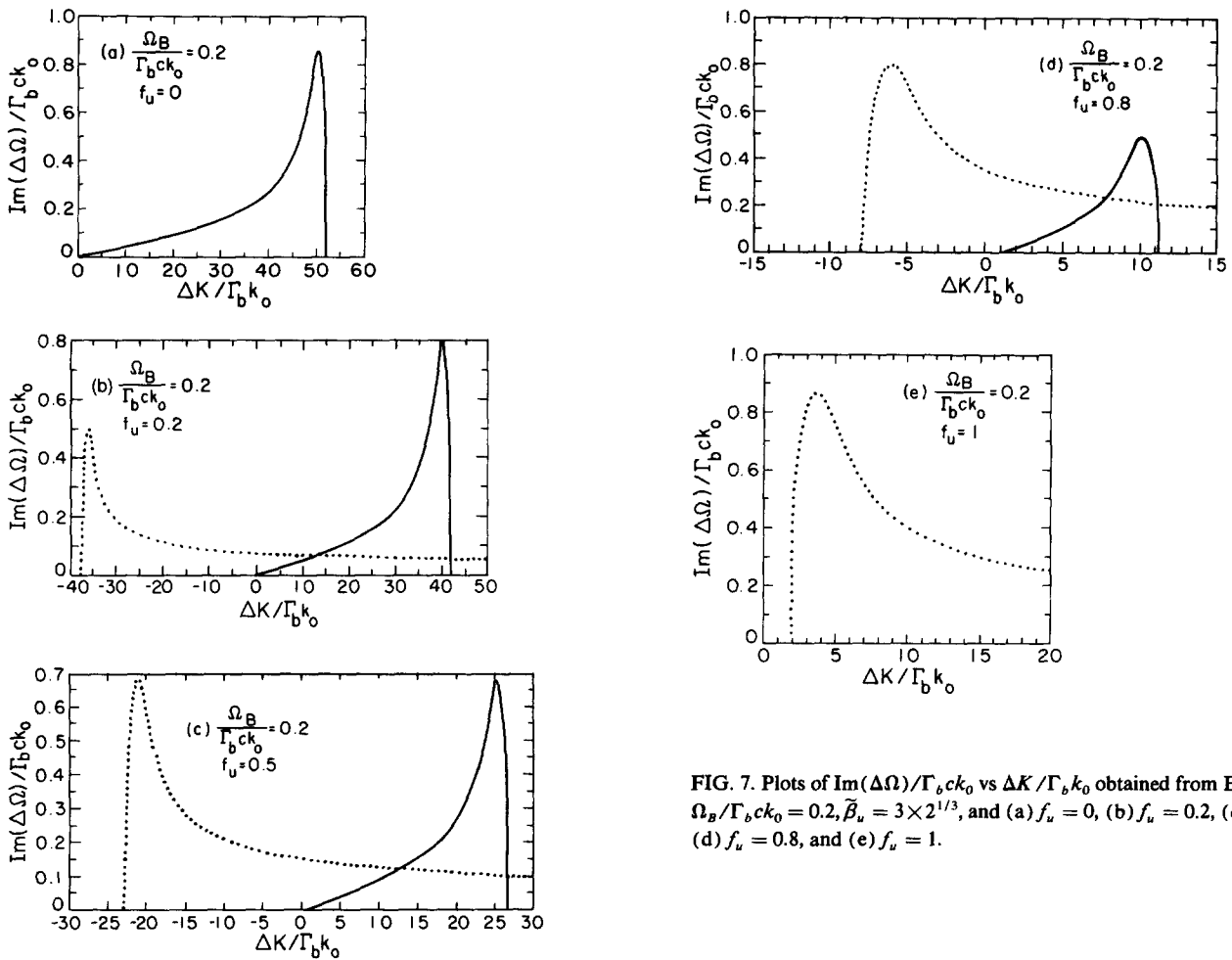


FIG. 7. Plots of $\text{Im}(\Delta\Omega)/\Gamma_b ck_0$ vs $\Delta K/\Gamma_b k_0$ obtained from Eq. (86) for $\Omega_B/\Gamma_b ck_0 = 0.2$, $\tilde{\beta}_u = 3 \times 2^{1/3}$, and (a) $f_u = 0$, (b) $f_u = 0.2$, (c) $f_u = 0.5$, (d) $f_u = 0.8$, and (e) $f_u = 1$.

ing in mind the symmetries in Eq. (87) and Fig. 3, throughout the remainder of this paper we display only the stability results corresponding to the rightmost growth curves in Figs. 3(a) and 3(c). That is, in Figs. 4–8, the stability results are presented only for the rightmost lobes of the growth rate curves. With populations of both trapped and untrapped electrons, it is found that the untrapped-electron mode corresponding to the rightmost lobe in Fig. 3(a) can exhibit growth for negative as well as positive values of ΔK . This effect is most pronounced at small values of $\Omega_B/\Gamma_b ck_0$ (see Figs. 6 and 7).

Figure 4 shows plots of the normalized growth rate $\text{Im}(\Delta\Omega)/\Gamma_b ck_0$ vs $\Delta K/\Gamma_b k_0$ obtained from Eq. (86) for $\Omega_B/\Gamma_b ck_0 = 2^{1/3}$ and fraction of untrapped electrons ranging from $f_u = 0$ [Fig. 4(a)] to $f_u = 1$ [Fig. 4(e)]. For $f_u = 0$, Fig. 4(a) corresponds to the familiar growth rate curve^{37,73} for the sideband instability assuming a slowly varying equilibrium wave phase and that all of the electrons are deeply trapped. [Indeed, for $f_u = 0$ and $\tilde{\Omega}_B = 2^{1/3}$, Eq. (68) can be solved analytically,³⁷ which gives a useful calibration of the numerical results.] Adding an untrapped electron component, it is evident from Figs. 4(b)–4(e) that a new unstable mode (driven by the untrapped electrons) is introduced. The *untrapped-electron* mode is represented by the dotted curves in Figs. 4(b)–4(e), whereas the *sideband* mode is represented by the solid curves. As expected for zero energy spread, the untrapped-electron mode in Figs. 4(b)–

4(e) has a relatively broad bandwidth in ΔK space. Moreover, as f_u is increased (thereby decreasing the fraction of trapped electrons), the growth rate and bandwidth of the sideband instability continue to decrease as f_u is increased from $f_u = 0.2$ [Fig. 4(b)], to $f_u = 0.5$ [Fig. 4(c)], to $f_u = 0.8$ [Fig. 4(d)]. Indeed, for $f_u = 1$ (no trapped electrons), the sideband instability is completely absent (as expected), and only the instability driven by the untrapped electrons is present [Fig. 4(e)].

It is evident from Figs. 4(a)–4(e) that the properties of $\text{Im}(\Delta\Omega)/\Gamma_b ck_0$ vs $\Delta K/\Gamma_b k_0$ differ in detail for the two unstable modes. However, an equally striking feature of Fig. 4 is that the characteristic maximum growth rate of the most unstable mode varies by only a small amount (less than 25%) between the case where there are no untrapped electrons [$f_u = 0$ in Fig. 4(a)] to the case where there are no trapped electrons [$f_u = 1$ in Fig. 4(e)]. The present analysis suggests that the linear and nonlinear evolution of the beam electrons and radiation field may be substantially modified by the presence of an untrapped-electron component when $f_u \gtrsim 0.2$.

Figure 5 shows plots of the normalized real frequency $\text{Re}(\Delta\Omega)/\Gamma_b ck_0$ vs $\Delta K/\Gamma_b k_0$ obtained from Eq. (86) for $\Omega_B/\Gamma_b ck_0 = 2^{1/3}$, and $f_u = 0$ [Fig. 5(a)], $f_u = 0.5$ [Fig. 5(b)], and $f_u = 1$ [Fig. 5(c)]. The system parameters in Figs. 5(a), 5(b), and 5(c) are identical to Figs. 4(a), 5(c), and 5(e), respectively. Moreover, $\text{Re}(\Delta\Omega)$ is plotted only

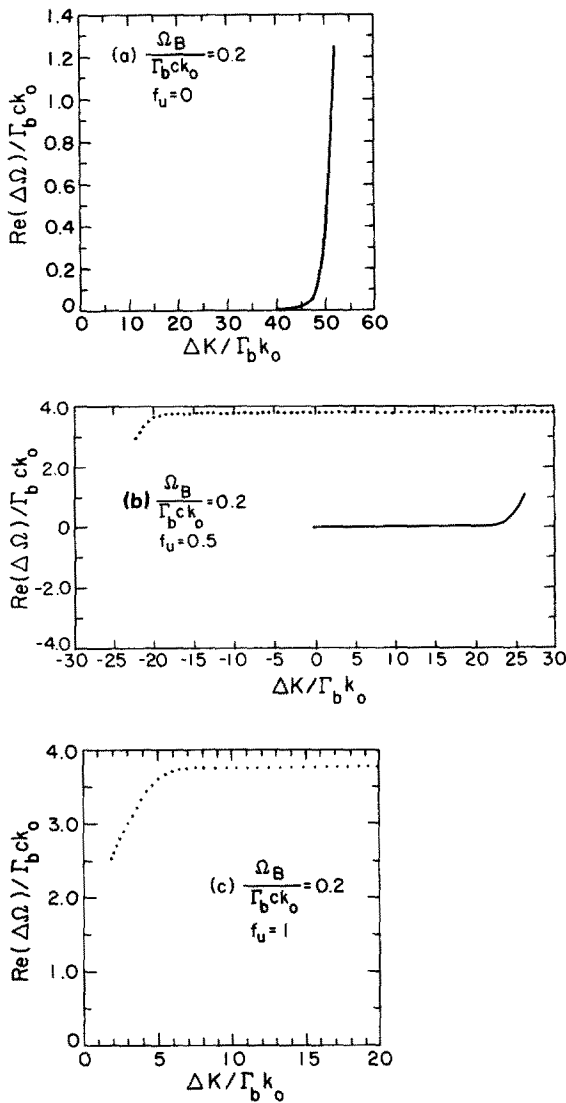


FIG. 8. Plots of $\text{Re}(\Delta\Omega)\Gamma_b ck_0$ vs $\Delta K/\Gamma_b k_0$ obtained from Eq. (86) for $\Omega_B/\Gamma_b ck_0 = 0.2$, $\beta_u = 3 \times 2^{1/3}$, and (a) $f_u = 0$, (b) $f_u = 0.5$, and (c) $f_u = 1$.

over the unstable range of ΔK , and the solid curves in Fig. 5 correspond to the sideband mode whereas the dotted curves correspond to the untrapped-electron mode. Evidently, $\text{Re}(\Delta\Omega)$ increases monotonically with ΔK for the sideband mode [Figs. 5(a) and 5(b)]. Furthermore, the magnitude of $\text{Re}(\Delta\Omega)$ is somewhat larger for the untrapped-electron mode [Figs. 5(b) and 5(c)]. Moreover, $\text{Re}(\Delta\Omega)$ is approximately constant for the untrapped-electron mode for ΔK in the range $\Delta K/\Gamma_b k_0 \gtrsim 5$.

In Fig. 6, the normalized pump strength is reduced to $\Omega_B/\Gamma_b ck_0 = 0.5$. In particular, Fig. 6 shows plots of the normalized growth rate $\text{Im}(\Delta\Omega)/\Gamma_b ck_0$ vs $\Delta K/\Gamma_b k_0$ obtained from Eq. (86) for $\Omega_B/\Gamma_b ck_0 = 0.5$ and fraction of untrapped electrons ranging from $f_u = 0$ [Fig. 6(a)] to $f_u = 1$ [Fig. 6(e)]. In Fig. 6, the general features of the growth rate curves for the sideband mode (solid curves) and the untrapped-electron mode (dotted curves) are qualitatively similar to those of Fig. 4, although the bandwidth of the sideband instability is considerably larger for the smaller value of $\Omega_B/\Gamma_b ck_0$ chosen in Fig. 6 [compare Figs. 4(a) and

6(a)]. Moreover, the maximum growth rate of the untrapped-electron mode shifts from negative values of ΔK for $f_u \lesssim 0.5$ [Figs. 6(b) and 6(c)] to positive values of ΔK for $f_u > 0.5$ [Figs. 6(d) and 6(e)]. As in Fig. 4, it is evident from Fig. 6 that the characteristic maximum growth rate of the most unstable mode varies by only a small amount over the entire range from $f_u = 0$ [Fig. 6(a)] to $f_u = 1$ [Fig. 6(e)]. However, the detailed properties of $\text{Im}(\Delta\Omega)/\Gamma_b ck_0$ vs $\Delta K/\Gamma_b k_0$ differ considerably for the two modes.

Finally, in Figs. 7 and 8, the normalized pump strength is reduced further to $\Omega_B/\Gamma_b ck_0 = 0.2$. Shown are plots of $\text{Im}(\Delta\Omega)/\Gamma_b ck_0$ (Fig. 7) and $\text{Re}(\Delta\Omega)/\Gamma_b ck_0$ (Fig. 8) vs $\Delta K/\Gamma_b k_0$ obtained from Eq. (86) for $\Omega_B/\Gamma_b ck_0 = 0.2$ and values of f_u ranging from $f_u = 0$ to $f_u = 1$. As in Figs. 4 and 6, only the sideband mode is unstable for $f_u = 0$ [Fig. 7(a)], whereas only the untrapped-electron mode is unstable for $f_u = 1$ [Fig. 7(e)]. Finally, as in Figs. 4 and 6, the characteristic maximum growth rate of the most unstable mode varies by only a small amount over the entire range of f_u considered in Fig. 7.

V. CONCLUSIONS

This paper has investigated the detailed influence of untrapped electrons on the sideband instability in a helical wiggler free electron laser. Small-amplitude perturbations are assumed about a constant-amplitude ($\hat{a}_s^0 = \text{const}$) primary electromagnetic wave with a slowly varying equilibrium phase δ_s^0 [Eqs. (40) and (41)]. A simple model is adopted in which all of the trapped electrons are deeply trapped, and the equilibrium motion of the untrapped electrons (assumed monoenergetic) is only weakly modulated by the ponderomotive potential. The theoretical model is based on the single-particle orbit equations together with Maxwell's equations and appropriate statistical averages (Sec. II). Like our recent treatment³⁷ of the sideband instability (which neglects the effects of untrapped electrons), the present analysis is carried out in the ponderomotive frame, which leads to a substantial simplification in deriving the dispersion relation (70) (Sec. III). Transforming Eq. (70) back to the laboratory-frame frequency $\omega = \omega_s + \Delta\omega$ and wavenumber $k = k_s + \Delta k$, detailed properties of the sideband instability are investigated, including the effects of the untrapped electrons (Sec. IV).

The resulting dispersion relation (86) has been analyzed numerically over a wide range of the dimensionless pump strength $\Omega_B/\Gamma_b ck_0$ and the fraction of untrapped electrons $f_u = \hat{n}_u/\hat{n}_b$. To summarize briefly, when both trapped electrons and untrapped electrons are present, there are generally two types of unstable modes, which we refer to as the sideband mode, and the untrapped-electron mode. For $f_u = 0$, only the sideband instability is present (as expected). As f_u is increased, the growth rate of the sideband instability decreases, whereas the growth rate of the untrapped-electron mode increases until only the untrapped-electron mode is unstable for $f_u = 1$ (Figs. 4, 6, and 7).

It is evident from the present analysis that the detailed growth properties are quite different for the two unstable modes. However, a very important feature of the stability results is that the characteristic maximum growth rate of the

most unstable mode varies by only a small amount over the entire range of f_u from $f_u = 0$ (no untrapped electrons) to $f_u = 1$ (no trapped electrons). The present analysis suggests that the linear and nonlinear evolution of the beam electrons and radiation field may be substantially modified by the presence of an untrapped-electron component when $f_u \gtrsim 0.2$.

ACKNOWLEDGMENTS

This research was supported in part by the Office of Naval Research and in part by the National Science Foundation.

- ¹N. M. Kroll and W. A. McMullin, *Phys. Rev. A* **17**, 300 (1978).
- ²A. Hasegawa, *Bell Syst. Tech. J.* **57**, 3069 (1978).
- ³W. B. Colson, *Phys. Lett. A* **59**, 187 (1976).
- ⁴V. P. Sukhatme and P. A. Wolff, *J. Appl. Phys.* **44**, 2331 (1973).
- ⁵C. A. Brau, *IEEE J. Quantum Electron.* **QE-21**, 824 (1985).
- ⁶R. W. Warren, B. E. Newnam, and J. C. Goldstein, *IEEE J. Quantum Electron.* **QE-21**, 882 (1985).
- ⁷T. J. Orzechowski, B. Anderson, W. M. Fawley, D. Prosnitz, E. T. Scharlemann, S. Yarema, D. B. Hopkins, A. C. Paul, A. M. Sessler, and J. S. Wurtele, *Phys. Rev. Lett.* **54**, 889 (1985).
- ⁸T. J. Orzechowski, E. T. Scharlemann, B. Anderson, V. K. Neil, W. M. Fawley, D. Prosnitz, S. M. Yarema, D. B. Hopkins, A. C. Paul, A. M. Sessler, and J. S. Wurtele, *IEEE J. Quantum Electron.* **QE-21**, 831 (1985).
- ⁹M. Billardon, P. Elleaume, J. M. Ortega, C. Bazin, M. Bergher, M. Velghe, D. A. G. Deacon, and Y. Petroff, *IEEE J. Quantum Electron.* **QE-21**, 805 (1985).
- ¹⁰J. Masud, T. C. Marshall, S. P. Schlesinger, and F. G. Yee, *Phys. Rev. Lett.* **56**, 1567 (1986).
- ¹¹J. Fajans, G. Bekefi, Y. Z. Yin, and B. Lax, *Phys. Rev. Lett.* **53**, 246 (1984).
- ¹²R. W. Warren, B. E. Newnam, J. G. Winston, W. E. Stein, L. M. Young, and C. A. Brau, *IEEE J. Quantum Electron.* **QE-19**, 391 (1983).
- ¹³G. Bekefi, R. E. Shefer, and W. W. Destler, *Appl. Phys. Lett.* **44**, 280 (1983).
- ¹⁴C. W. Roberson, J. A. Pasour, F. Mako, R. F. Lucey, Jr., and P. Sprangle, *Infrared Millimeter Waves* **10**, 361 (1983), and references therein.
- ¹⁵A. Grossman, T. C. Marshall, and S. P. Schlesinger, *Phys. Fluids* **26**, 337 (1983).
- ¹⁶D. Prosnitz and A. M. Sessler, in *Physics of Quantum Electronics* (Addison-Wesley, Reading, MA, 1982), Vol. 9, p. 651.
- ¹⁷R. K. Parker, R. H. Jackson, S. H. Gold, H. P. Freund, V. L. Granatstein, P. C. Efthimion, M. Herndon, and A. K. Kinkead, *Phys. Rev. Lett.* **48**, 238 (1982).
- ¹⁸S. Benson, D. A. G. Deacon, J. N. Eckstein, J. M. J. Madey, K. Robinson, T. I. Smith, and R. Taber, *Phys. Rev. Lett. A* **48**, 235 (1982).
- ¹⁹A. N. Didenko, A. R. Borisov, G. R. Fomenko, A. V. Kosevnikov, G. V. Melnikov, Yu G. Stein, and A. G. Zerlitsin, *IEEE Trans. Nucl. Sci.* **NS-28**, 3169 (1981).
- ²⁰D. B. McDermott, T. C. Marshall, S. P. Schlesinger, R. K. Parker, and V. L. Granatstein, *Phys. Rev. Lett.* **41**, 1368 (1978).
- ²¹D. A. G. Deacon, L. R. Elias, J. M. J. Madey, G. J. Ramian, H. A. Schwettman, and T. I. Smith, *Phys. Rev. Lett.* **38**, 892 (1977).
- ²²L. R. Elias, W. M. Fairbank, J. M. J. Madey, H. A. Schwettman, and T. I. Smith, *Phys. Rev. Lett.* **36**, 717 (1976).
- ²³R. C. Davidson, *Phys. Fluids* **29**, 2689 (1986).
- ²⁴R. C. Davidson, J. S. Wurtele, and R. E. Aamodt, *Phys. Rev. A* **34**, 3063 (1986).
- ²⁵B. Lane and R. C. Davidson, *Phys. Rev. A* **27**, 2008 (1983).
- ²⁶A. M. Dimos and R. C. Davidson, *Phys. Fluids* **28**, 677 (1985).
- ²⁷R. C. Davidson and Y. Z. Yin, *Phys. Fluids* **28**, 2524 (1985).
- ²⁸T. Taguchi, K. Mima, and T. Mochizuki, *Phys. Rev. Lett.* **46**, 824 (1981).
- ²⁹F. A. Hopf, P. Meystre, M. O. Scully, and W. H. Louisell, *Phys. Rev. Lett.* **37**, 1342 (1976).
- ³⁰R. C. Davidson and W. A. McMullin, *Phys. Rev. A* **26**, 410 (1982).
- ³¹N. S. Ginzburg and M. A. Shapiro, *Opt. Commun.* **40**, 215 (1982).
- ³²J. C. Goldstein and W. B. Colson, in *Proceedings of the International Conference on Lasers* (STS, McLean, VA, 1982), p. 218.
- ³³W. B. Colson, *IEEE J. Quantum Electron.* **QE-17**, 1417 (1981).
- ³⁴P. Sprangle, C. M. Tang, and W. M. Manheimer, *Phys. Rev. A* **21**, 302 (1980).
- ³⁵W. H. Louisell, J. F. Lam, D. A. Copeland, and W. B. Colson, *Phys. Rev. A* **19**, 288 (1979).
- ³⁶N. M. Kroll, P. L. Morton, and M. N. Rosenbluth, *IEEE J. Quantum Electron.* **QE-17**, 1436 (1981).
- ³⁷R. C. Davidson and J. S. Wurtele, *Phys. Fluids* **30**, 557 (1987).
- ³⁸D. C. Quimby, J. M. Slater, and J. P. Wilcoxon, *IEEE J. Quantum Electron.* **QE-21**, 979 (1985).
- ³⁹N. S. Ginzburg and M. I. Petelin, *Int. J. Electron.* **59**, 291 (1985).
- ⁴⁰C. M. Tang and P. Sprangle, in *Free Electron Generators of Coherent Radiation*, edited by C. A. Brau, S. F. Jacobs, and M. O. Scully (Society for Optical Engineers, Bellingham, WA, 1983), Vol. 453, p. 11.
- ⁴¹R. A. Freedman and W. B. Colson, *Opt. Commun.* **52**, 409 (1985).
- ⁴²W. B. Colson, *Nucl. Instrum. Methods in Phys. Res. A* **250**, 168 (1986).
- ⁴³M. N. Rosenbluth, H. V. Wong, and B. N. Moore, in *Ref. 40*, p. 25.
- ⁴⁴A. T. Lin, *Phys. Quantum Electron.* **9**, 867 (1982).
- ⁴⁵H. Al-Abawi, J. K. McIver, G. T. Moore, and M. O. Scully, *Phys. Quantum Electron.* **8**, 415 (1982).
- ⁴⁶W. B. Colson, *Phys. Quantum Electron.* **8**, 457 (1982).
- ⁴⁷J. Goldstein, in *Ref. 40*, p. 2.
- ⁴⁸R. C. Davidson and Y. Z. Yin, *Phys. Rev. A* **30**, 3078 (1984).
- ⁴⁹G. L. Johnston and R. C. Davidson, *J. Appl. Phys.* **55**, 1285 (1984).
- ⁵⁰H. P. Freund and A. K. Ganguly, *Phys. Rev. A* **28**, 3438 (1983).
- ⁵¹H. S. Uhm and R. C. Davidson, *Phys. Fluids* **26**, 288 (1983).
- ⁵²R. C. Davidson and H. S. Uhm, *J. Appl. Phys.* **53**, 2910 (1982).
- ⁵³H. S. Uhm and R. C. Davidson, *Phys. Fluids* **24**, 2348 (1981).
- ⁵⁴R. C. Davidson, W. A. McMullin, and K. Tsang, *Phys. Fluids* **27**, 233 (1983).
- ⁵⁵R. C. Davidson and W. A. McMullin, *Phys. Fluids* **26**, 840 (1983).
- ⁵⁶W. A. McMullin and G. Bekefi, *Phys. Rev. A* **25**, 1826 (1982).
- ⁵⁷R. C. Davidson and W. A. McMullin, *Phys. Rev. A* **26**, 1997 (1982).
- ⁵⁸W. A. McMullin and G. Bekefi, *Appl. Phys. Lett.* **39**, 845 (1981).
- ⁵⁹R. C. Davidson, *Phys. Fluids* **29**, 267 (1986).
- ⁶⁰R. C. Davidson and J. S. Wurtele, *IEEE Trans. Plasma Sci.* **PS-13**, 464 (1985).
- ⁶¹H. P. Freund, R. A. Kehs, and V. L. Granatstein, *IEEE J. Quantum Electron.* **QE-21**, 1080 (1985).
- ⁶²H. P. Freund and A. K. Ganguly, *IEEE J. Quantum Electron.* **QE-21**, 1073 (1985).
- ⁶³B. Hafizi and R. E. Aamodt, *Phys. Rev. A* **29**, 2656 (1984).
- ⁶⁴P. Sprangle, C. M. Tang, and I. Bernstein, *Phys. Rev. A* **28**, 2300 (1983).
- ⁶⁵H. P. Freund and P. Sprangle, *Phys. Rev. A* **28**, 1835 (1983).
- ⁶⁶R. C. Davidson and H. S. Uhm, *Phys. Fluids* **23**, 2076 (1980).
- ⁶⁷P. Sprangle and R. A. Smith, *Phys. Rev. A* **21**, 293 (1980).
- ⁶⁸I. B. Bernstein and J. L. Hirshfield, *Physica A (Utrecht)* **20**, 1661 (1979).
- ⁶⁹T. Kwan and J. M. Dawson, *Phys. Fluids* **22**, 1089 (1979).
- ⁷⁰T. Kwan, J. M. Dawson, and A. T. Lin, *Phys. Fluids* **20**, 581 (1977).
- ⁷¹A. Bambini and A. Renieri, *Lett. Nuovo Cimento* **21**, 399 (1978).
- ⁷²S. T. Stenholm and A. Bambini, *IEEE J. Quantum Electron.* **QE-17**, 1363 (1981).
- ⁷³M. N. Rosenbluth (private communication, 1986).